

Optimization and Longevity of Functionalized Multi-Walled Carbon Nanotube-Enabled
Membranes for Water Treatment

A Thesis
presented to
the Faculty of California Polytechnic State University,
San Luis Obispo

In Partial Fulfillment
of the Requirements for the Degree
Master of Science in Civil and Environmental Engineering

By
Madeleine M. White
June 2020

© 2020
Madeleine M. White
ALL RIGHTS RESERVED

COMMITTEE MEMBERSHIP

TITLE: Optimization and Longevity of Functionalized
Multi-Walled Carbon Nanotube-Enabled
Membranes for Water Treatment

AUTHOR: Madeleine M. White, EIT

DATE SUBMITTED: June 2020

COMMITTEE CHAIR: Rebekah Oulton, Ph.D.
Associate Professor of Civil &
Environmental Engineering

COMMITTEE MEMBER: Trygve Lundquist, Ph.D.
Professor of Environmental
Engineering

COMMITTEE MEMBER: Amr El Badawy, Ph.D.
Assistant Professor of Environmental
Engineering

ABSTRACT

Optimization and Longevity of Functionalized Multi-Walled Carbon Nanotube-Enabled Membranes for Water Treatment

Madeleine M. White

Water scarcity is a growing concern at the global scale. Large scale water reuse is growing both in necessity and popularity. Before water reuse can be performed efficiently on a large scale or be used for potable supply, even indirectly, contaminants of emerging concern (CECs) will need to be treated at the full scale. Advanced oxidation processes (AOPs) are a form of advanced water treatment capable of treating a wide range of CECs. This study contributes to the growing field of AOPs and more specifically AOPs using ozone combined with functionalized multi-walled carbon nanotubes (MWCNTs). Ozonation of MWCNTs has been found to increase hydroxyl radical production and improve AOP treatment. Novel MWCNT-enabled membranes were used as catalysts for ozonation to degrade the CEC Atrazine. Atrazine is an ozone recalcitrant CEC that is commonly found in herbicides. Atrazine removal results, found using a high-performance liquid chromatograph (HPLC), were inconsistent between membranes constructed using identical procedures. Further analysis using Fourier transform infrared (FTIR) spectroscopy, scanning electron microscopes (SEM), and UV-Vis spectrophotometry was conducted to explore inconsistencies in construction of the membranes which might explain removal inconsistencies and predict membrane longevity. Removal was found to be influenced by filtration time and ozone exposure. Ozone exposure and filtration time influence percent removal because they both affect hydroxyl formation. The membrane test filtration duration, for equal filtered volumes, ranged from under 5 minutes to nearly an hour. It is believed that filtration time inconsistency was due to inconsistent MWCNT loading on the surface of the membranes. Extended exposure to ozone might change the surface chemistry of the MWCNTs on the membrane surface, affecting hydroxyl radical production. Additionally, repeated use of the membrane created surface defects that might reduce the membrane strength. This study found that the lifetime of the membrane is far past what was simulated in lab and further testing must be performed.

ACKNOWLEDGMENTS

I would like to acknowledge and thank the following for the roles they have played in supporting me finish my degree.

Dr. Rebekah Oulton, not only has she been an irreplaceable advisor and mentor, she has been the source of many smiles during my time at Cal Poly. Her extensive knowledge and endless hunger for knowledge has made this experience possible. Thank you for your guidance and support.

Dr. Trevor Harding for his welcoming nature and overwhelming support. Dr. Harding single handedly guided me in using materials engineering resources and interpreting my research.

Dr. Trygve Lundquist and Dr. Amr El Badawy and the many other Environmental and Civil Engineering professors who have been a valuable resource to my learning and development as a student.

Graduates Emily Miller and Kelly Cochran for allowing me to shadow them during their research.

My fellow peers for making the hours of studying and writing a little less lonely.

My friends and family across the nation who believed in me, listened to many research related rants, and provided me with love and support.

TABLE OF CONTENTS

LIST OF FIGURES	x
CHAPTER	
1. INTRODUCTION.....	1
1.1 Research Questions	2
2. LITERATURE REVIEW	4
2.1 Emerging Contaminants and Breakdown Products	5
2.2 Atrazine	5
2.3 Conventional Treatment Processes	8
2.4 Primary and Secondary Treatment	9
2.5 Advanced Treatment Processes.....	10
2.5.1 Membrane Filtration.....	10
2.5.2 Activated Carbon	12
2.5.3 Direct Oxidation	13
2.6 Advanced Oxidation Processes	13
2.6.1 Carbon Nanotubes and Ozone.....	15
2.7 Nano-Enabled Material.....	17
2.7.1 Practical Applications.....	17
2.8 Fourier Transform Infrared Spectroscopy	18

2.10 Electron Microscopy	22
2.11 SEM & TEM Results for CNTs	23
2.12 UV-Vis Spectroscopy	25
2.12.1 UV-Vis Results for CNTs	25
3. METHODS.....	27
3.1 CNT Functionalization Procedure	27
3.2 Bucky Method	28
3.3 CNT Membrane Lab Testing Procedure	28
3.3.1 Atrazine Solution.....	28
3.3.2 Phosphate Buffer	28
3.3.3 Sodium Sulfite Solution.....	29
3.3.4 Ozone	29
3.3.5 Vacuum Filter Process.....	30
3.3.6 Analysis for CNT Membrane Lab Testing	31
3.3.7 Quality Assurance and Analysis of Filtration and HPLC Procedure	31
3.4 FTIR Procedure	32
3.4.1 Quality Assurance and Analysis of FTIR Procedure	32
3.5 Scanning Electron Microscope Procedure	32
3.5.1 Quality Assurance and Analysis of SEM Procedure	33
3.6 UV- Vis Procedure	34

3.6.1 Quality Assurance and Analysis of UV-Vis Procedure.....	34
4. RESULTS AND DISCUSSION	35
4.1 Percent Removal	35
4.1.1 Relative humidity and ambient temperature	35
4.1.2 Filtration Time	38
4.1.3 Steady-State Ozone Concentration	39
4.1.4 Ozone Exposure	40
4.1.5 Repeated Uses of Filter	41
4.1.6 Total Ozone Exposure	42
4.2 Membrane Longevity	45
4.2.1 Scanning Electron Microscopy	45
4.2.2 Filtration Time	52
4.2.3 Total Ozone Exposure	56
5. CONCLUSIONS AND FUTURE WORK	60
5.1 Percent Removal	60
5.2 Membrane Longevity	61
5.3 Membrane Variability	63
5.4 Future Work	63
5.4.1 Improved Membrane Fabrication Procedure	63
5.4.2 Further Membrane Longevity Testing	64

5.4.3 Safety Concerns	64
5.4.4 The Future of Advanced Water Treatment	65
REFERENCES	66
APPENDICES	70
Appendix A: FTIR ATR Software Instructions	70
Appendix B: Percent Removal Results Including all Membrane 6 Values	77
Appendix C: Additional SEM Images of Membrane 3B and 5.....	81

LIST OF FIGURES

Figure	Page
Figure 1: Photosynthesis and the Hill reaction at the thylakoid membrane [5].	6
Figure 2: Metabolic pathway followed by Atrazine during degradation [10].	7
Figure 3: Schematic of Flow-through system. Schematic created by Jason Haas, Adopted from Oulton. [15]	18
Figure 4: FTIR example spectra. [18]	19
Figure 5: FTIR-ATR figure depicting reflectance off a sample [21].	20
Figure 6: Spectra labeling common functional groups [22].	20
Figure 7: Functionalized samples, FTIR spectra of P-MWNT, F-MWNT-1 h, F- MWNT-2 h, and F-MWNT-4 h, FTIR spectra [23].	21
Figure 8: SEM of MWCNTs: (a) pristine A-type MWCNTs, (b) A-type f-MWCNTs (HNO ₃), (c) A-type fMWCNTs (NH ₄ OH + H ₂ O ₂), (d) pristine P-type MWCNTs, (e) P-type f-MWCNTs (HNO ₃), (f) P-type fMWCNTs (NH ₄ OH + H ₂ O ₂) [26].	23
Figure 9: Representative TEM Micrographs (left to right): pristine MWCNTs (0.9% O), H ₂ O ₂ treated MWCNTs (4.5% O), H ₂ SO ₄ /HNO ₃ treated MWCNTs (5.1% O), KMnO ₄ treated MWCNTs (5.3% O). Amorphous carbon is indicated with arrows, sidewall defects highlighted by circles [24].	24
Figure 10: The UV–Vis spectrum of P-MWNTs and F-MWNT-2 h in water after half an hour and 20 days of 5 min ultrasonic mixing [23]	26
Figure 11: Vacuum filtration process under fume hood.	31
Figure 12: Membrane 3B (on left) and Membrane 5 adhered to 12 mm aluminum stubs.	33
Figure 13: Percent relative humidity compared to ozone absorbance.	36
Figure 14: Ambient temperature compared to ozone absorbance.	37
Figure 15: Relative humidity compared to percent contaminant removal.	37
Figure 16: Ambient temperature compared to percent contaminant removal.	38
Figure 17: Filtration time compared to percent contaminant removal.	39

Figure 18: Ozone absorbance in solution compared to percent contaminant removal.	39
Figure 19: Ozone exposure in solution compared to percent contaminant removal.	41
Figure 20: Number of samples filtered compared to percent contaminant removal.	42
Figure 21: Ozone exposure over the life of the membrane compared to percent contaminant removal.	43
Figure 22: Compilation of notable results from filtration tests.	44
Figure 23: Number of samples filtered compared to filtration time.	45
Figure 24: Picture of membranes chosen for SEM imaging.	46
Figure 25: SEM image of membrane 3B, photo 2 of 5.	47
Figure 26: SEM image of membrane 3B, photo 1 of 5.	48
Figure 27: SEM image of membrane 5, photo 1 of 5.	49
Figure 28: SEM image of membrane 5, photo 2 of 5.	49
Figure 29: SEM image of membrane 2B.	50
Figure 30: Low magnification TEM micrographs (left to right): pristine MWCNTs (0.9% O), O ₃ treated MWCNTs (4.7% O), H ₂ SO ₄ /HNO ₃ treated MWCNTs (10.2% O) [24].	51
Figure 31: Representative TEM Micrographs (left to right): pristine MWCNTs (0.9% O), H ₂ O ₂ treated MWCNTs (4.5% O), H ₂ SO ₄ /HNO ₃ treated MWCNTs (5.1% O), KMnO treated MWCNTs (5.3% O). Amorphous carbon is indicated with arrows, sidewall defects highlighted by circles [24].	52
Figure 32: UV-Vis spectra from functionalized MWCNTs in solution.	53
Figure 33: SEM image of membrane 2B, photo 1 of 2.	54
Figure 34: SEM image of membrane 2B, photo 2 of 2.	55
Figure 35: SEM image of membrane 5, photo 3 of 5.	55
Figure 36: SEM image of membrane 5, photo 2 of 5.	56
Figure 37: Membrane ozone exposure compared to filtration time.	57
Figure 38: FTIR spectra of nylon membrane blank.	58

Figure 39: a) FTIR spectra of functionalized membrane 4 (top). b) FTIR spectra of non-functionalized membrane (bottom)..... 59

1. INTRODUCTION

Access to potable water is a timeless issue. Growing populations worldwide have further increased demand for water resources. Given the high costs of imported water and seawater desalination, advanced water treatment (AWT) to recycled water has come to the forefront of the conversation about how to sustain populations and ecosystems in arid and water-stressed regions. Indirect and direct potable reuse (IPR and DPR), that is the treatment of wastewater effluent to drinking water standards with or without the use of an environmental buffer, is a new water reuse technique that could decrease demand on depleted surface and groundwater.

One concern for both IPR and DPR is the addition of recalcitrant contaminants of emerging concern (CECs) with every cycle of reuse [1]. CECs include pharmaceuticals and personal care products (PPCPs), which are currently detectable at the parts per trillion (PPT) range in drinking water systems. Wastewater concentrations of PPCPs have been recorded between 0.1 and 100,000 PPT prior to treatment, though their effects on human health and the environment are not exactly known [15]. DPR would not provide a closed loop, because advanced treatment cannot achieve 100% water recovery; the drinking water from DPR would need to be supplemented from another source, such as the buffering reservoir of IPR. The consequence of using DPR or IPR for any fraction of drinking water is the accumulation of PPCPs overtime; treatment for CECs must be included in any DPR or IPR application. Technologies designed to treat CECs are growing in numbers and feasibility [1]. The present study aims to contribute to the growing field of advanced treatment processes aimed at treating CECs.

1.1 Research Questions

Results from previous studies, conducted by Dr. Rebekah Oulton and graduate students Kelly Cochran and Emily Miller of Cal Poly, San Luis Obispo, have contributed to the growing research into advanced oxidation processes (AOPs). Their research testing ozonation of MWCNTS as an AOP in batch or semi-batch reactor systems have produced promising results. However, due to the variability of ozone concentration with respect to time and volumetric inefficiencies, a batch reactor is an infeasible form of treatment large scale.

More recent studies have been conducted using a continuous ozonation flow through MWCNT-embedded membrane technique [15]. The flow through technique has been found to be extremely inconsistent with respect to ozone concentration, contaminant removal efficiency, and retention time.

The present study repeats and builds on previous studies using continuous ozonation flow through membrane technique in hopes of identifying those variables with greatest effect on contaminant removal. In addition, this study explores qualitative differences between membranes at different stages of use/ treatment, to determine how membrane efficacy changes with repeated use. Qualitative methods included Fourier transform infrared spectroscopy (FTIR) to evaluate the surface chemistry of the multi-walled carbon nanotube (MWCNT)-enabled membrane after repeated uses. Furthermore, a scanning electron microscope (SEM) provided visual imaging of the membrane's surface. UV-Vis spectrophotometry was used to evaluate light transmittance in a functionalized MWCNT solution. The results of this study intended to answer the following questions:

- What experimental and operational variables affect contaminant removal during a single pass through a CNT-enabled membrane during ozonating conditions?
- How do the CNT-enabled membranes change with repeated uses and extended exposure to ozone, specifically regarding surface functionalization of the CNTs and integrity of the membrane itself?
- Can these results explain the variability of results between different membranes prepared under identical conditions in prior studies?

1.2 General Approach

This study was designed to repeat methods performed previously using a MWCNT-enabled membrane in an ozonated vacuum filter to treat Atrazine. Furthermore, this study intends to discover potential causes for variability between different membranes that have been prepared using identical procedure using microscopy, spectroscopy, and spectrophotometry. Fourier Transform Infrared Spectroscopy was used to discover what functional groups were present on the surface of membranes following repeated use. A scanning electron microscope was used to take images of membranes representative of different levels of treatment. These images should illustrate surface flaws, preferential pathways, and changes to the surface caused by extended exposure to ozone. Lastly, UV-Vis spectrophotometry was used to identify transmittance of functionalized MWCNT solutions.

2. LITERATURE REVIEW

Implementation of direct and indirect potable reuse continues to rise as water scarcity remains a growing concern. One concern with DPR is the “closed-loop” nature of the water system, leading to higher concentrations of contaminants of emerging concern (CECs). The term “contaminants of emerging concern” refers to synthetic or naturally occurring chemicals or microorganisms in the environment “that have known or suspected adverse ecological and/or human health effects” [1]. Some CECs are more reactive to different forms of treatment than others. Atrazine is one of many CECs that are resistant to conventional treatment methods, and for this reason it is a useful indicator of the efficacy of an advanced treatment process.

Conventional water treatment includes preliminary, primary, secondary and sometimes tertiary or advanced treatment methods. Depending on the required effluent quality different treatment techniques can be chosen. To treat most CECs, advanced treatment methods are required. Such advanced treatment includes membrane filtration, adsorption and or oxidation processes. Ozone coupled with functionalized multiwalled carbon nanotubes (MWCNTs) is sufficient in producing oxygen functional groups capable of breaking down CECs. Qualitative and quantitative research methods are valuable in identifying removal efficiency and longevity of such membranes following repeated exposure to an oxidant.

2.1 Emerging Contaminants and Breakdown Products

CECs include pharmaceuticals, pesticides, industrial chemicals, surfactants, gasoline additives and personal care products. Emerging contaminant sources vary in rate of production and nature of production. Pollutant sources are classified as point and or non-point sources. Point sources include wastewater treatment plants, drug manufacturing industries, hospitals, livestock farms, aquaculture, household outflow etc. Non-Point sources are harder to identify; they include storm-water runoff, terrestrial runoff from roads, urban areas and agriculture land [2]. In surface waters, concentrations of the CECs have been found at a few hundred nanograms per liter or more [3].

A contaminant's persistence in the environment correlates with its accumulation in the environment over time. Bioaccumulation that occurs in the environment can raise concentrations to toxic levels. Emerging contaminant effects on humans are still largely unknown. However, their increasing presence poses potential for harm to humans and definite risk to aquatic life and amphibians [4]. When studying CECs, it is important to identify specific contaminants that are resistant to current treatments and therefore are more likely to escape into the environment.

2.2 Atrazine

Atrazine is a CEC, and more specifically an endocrine disruptor (aka endocrine disrupting compound or EDC). Endocrine disruptors alter the normal functions and production of hormones. Any part of the body that is affected by hormones can be affected by

endocrine disruptors. Endocrine disruptors can increase risk of tumors, birth defects and developmental disorders [6].

Atrazine is an herbicide of the Triazine class. Triazine class herbicides work by inhibiting photosynthesis. Specifically, this powerful herbicide interferes with the Hill reaction, a water splitting reaction that results in the production of free oxygen by plants. Photosynthesis begins with photosystem II, a protein complex that facilitates photosynthesis, it is this protein complex that Atrazine inhibits the entire reaction [5].

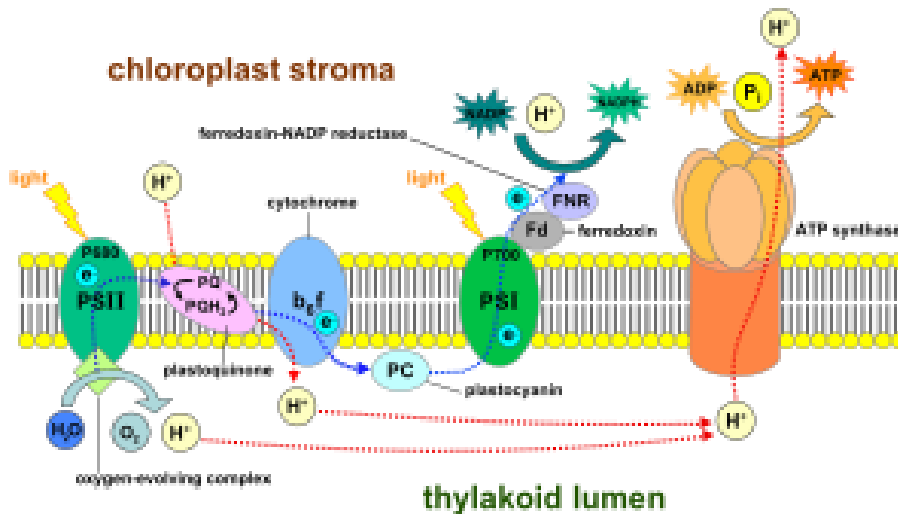


Figure 1: Photosynthesis and the Hill reaction at the thylakoid membrane [5].

Atrazine can be found, at varying concentrations, in Vigoro, Monsanto and Scotts Bonus consumer products [6]. In a 2018 U.S. Environmental Protection Agency (EPA) Human Health Risk Assessment, it was concluded that Atrazine does not pose any “dietary (food), residential handler, non-occupational spray drift, or occupational post-application” risks under registered uses [6]. Unlike the United States, many nations in Europe have more stringent laws around the use of Atrazine. Atrazine’s “long-term persistence in the environment, together with toxicity to wildlife and possible link to human health”

ultimately led to a European Union-wide ban in 2004 [30]. While still considering it safe, the U.S. EPA warns, outside of registered uses Atrazine can still pose a risk.

The maximum contaminant level (MCL) for Atrazine set by the United States EPA for drinking water is 3 ppb [7]. Atrazine rarely meets or exceeds EPA's drinking water standard, but it is often surpassed in surface water monitoring data, likely due to runoff from agricultural application. In 2017 Atrazine monitoring program data, 128 sites met or exceeded 3 ppb. The highest exceedances occurred in Ohio, Illinois, Kansas, Tennessee and Kentucky [8]. These areas are all known for a large agriculture footprint, which suggests a relationship between exceedances and the agriculture industry.

Due to Atrazine's low solubility (K_{sp} of 33,000 ppm), it has a low biodegradation rate and tends to persist in the environment. Atrazine contains an oxidized ring of carbon that is a poor source of energy for microorganisms (Figure 2). Atrazine degradation typically follows a metabolic pathway in which the carbon ring is fully oxidized and is a nitrogen source for aerobic microorganisms (Figure 2) [9].

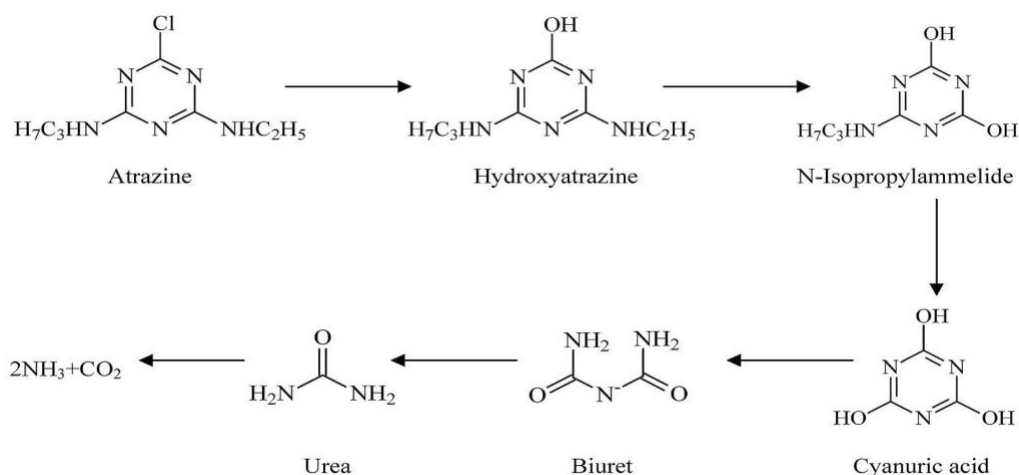


Figure 2: Metabolic pathway followed by Atrazine during degradation [10].

Atrazine's commercial use, persistence, and potential health risks increase the urgency to research removal techniques in drinking water and potable reuse systems. As it stands, Atrazine is recalcitrant to breakdown during conventional wastewater treatment. Atrazine is one of many persistent CECs that are resistant to conventional treatment. Studying impacts of AOPs on atrazine may provide insight into techniques that can be used for other CECs.

2.3 Conventional Treatment Processes

Wastewater treatment processes remove constituents via physical, chemical and biological methods. Physical treatment includes processes such as screening, mixing, flocculation, sedimentation, flotation, filtration and adsorption [11]. Chemical treatment removes constituents with the addition of chemicals or through chemical reactions. Examples of chemical treatment include precipitation, gas transfer, adsorption, and disinfection [11]. Biological treatment targets colloidal or biodegradable substances found in the water using microbes that break down these constituents. Biological treatment is typically performed by converting these biodegradable substances into gases that can escape, or into biological cell tissue that can be settled or separated physically [11]. Understanding the different levels of water treatment and their capability to remove CECs is important in designing a reliable system for potable water reuse.

2.4 Primary and Secondary Treatment

Water treatment is divided into preliminary, primary treatment, secondary treatment, tertiary treatment, advanced treatment and disinfection. Preliminary treatment is the initial treatment performed to remove large constituents that may cause maintenance or operational problems to later treatment processes [11]. Primary treatment performs initial removal of suspended solids and organic matter from the wastewater [11]. Secondary treatment removes biodegradable organics, suspended solids and nutrients. Disinfection is often included in the scope of secondary treatment [11]. Emerging contaminants are targeted in tertiary and advanced treatment. However, incidental CEC removal occurs during earlier stages.

During secondary treatment, conventional activated sludge (CAS) has been found to remove emerging contaminants. Removal efficiency via CAS is thought to be improved by modifying temperature and hydraulic and sludge retention time. Surfactant removal relies more heavily on sorption when residence time is too short for complete degradation. Pharmaceuticals, typically more polar pollutants, are more likely to be removed during biological transformation or mineralization induced by microorganisms [12]. Trickling filters are also capable of removing emerging contaminants though at a lower efficiency than CAS systems [15]. Endocrine disruptors, sunscreens and disinfectants, uniquely, have a higher removal rate by trickling filters than CAS systems. This is likely due to the trickling filter's ability to retain bacteria in the system, unlike CAS systems [15]. Immobilized bacteria populations in the trickling filter are "capable of degrading rather recalcitrant compounds" [15]. Both Primary and secondary treatment

processes are capable of degrading some CECs, however they should not be used as the primary removal system.

2.5 Advanced Treatment Processes

Following secondary treatment, effluent water contains a variety of trace constituents including both natural and synthetic organic chemicals at low levels. To protect human health and the environment, especially in potable reuse applications, additional treatment is required.

2.5.1 Membrane Filtration

Membrane filtration continues to grow in popularity as a form of advanced treatment. Membrane filtration is the process of using a semipermeable or osmotic driven membrane to remove particulate, colloidal and dissolved constituents from a liquid. Membrane filtration is able to remove a range of particle sizes typically from 0.0001 to 1.0 μm in diameter depending on the type of membrane[11]. The membrane pore size controls the passage of certain constituents and retention of others. From smallest to largest pore size, common membrane filtration processes include: microfiltration, ultrafiltration, nanofiltration and reverse osmosis. The driving force for the listed processes includes low and high-pressure systems [11]. Microfiltration and ultrafiltration require a low-pressure hydraulic force or vacuum, and nanofiltration and reverse osmosis require a high-pressure driving force [11].

Membrane technologies can be designed in different configurations out of various materials to be most efficient. Membrane units are constructed to account for membrane

type, pressure requirements, inlet and outlet feeds as well as overall support structure. Each unit design can be made to run water from the inside out or outside in. An outside-in flow is preferred because of its ability to run a backwash cycle. The membrane material depends on the type of membrane process and unit design. Membranes can be made from numerous organic or inorganic materials, most commonly polymers, ion exchange resin, ceramic or cellulose base [11]. The factors used to determine membrane material and unit design are fouling potential, deterioration, target constituents and results from pilot plant studies. Membrane filtration processes are typically paired with other treatment and pretreatment methods to improve efficiency and reduce fouling [13].

Ultra- and nanofiltration and reverse osmosis are capable of removing emerging contaminants. Membrane filtration rejects constituents due to pore size, adsorption and electrostatic repulsion. Ultrafiltration is the largest pore size capable of achieving some emerging contaminant removal. When mechanisms such as adsorption or electrostatic repulsion are the main mechanisms, membranes of a larger pore size can be used for retention of CECs [28]. Other physical factors relate to the retention achieved by membranes including hydrophobicity, surface roughness and relative charge. Furthermore, beyond the membrane, attributes of the feed water containing the CECs affect the membrane's ability to prevent pass-through [28]. Attributes that can affect the feed water and the membranes effectiveness include concentration of suspended and dissolved solids, pH and salinity. When designing a system intended to treat CECs, membrane technology can be a valuable asset.

2.5.2 Activated Carbon

Activated carbon is one of the principle materials for adsorption treatment. Activated carbon can be distinguished by two size classes: powdered activated carbon which is less than 0.074 mm in size and granular activated carbon which has a diameter of 0.1 mm or more [11].

Both sizes perform relatively the same process of adsorption. The adsorption process can be broken down into individual steps. The first step is bulk solution transport. During bulk solution transport, the organic material moves through the liquid to the boundary layer fixed film around the adsorbent, activated carbon. Next, the organic material diffuses through the fixed film layer to the pores of the adsorbent. Following, organic material moves through the pores via molecular diffusion through the liquid and or by diffusion along the surface of the adsorbent. The last step is adsorption of the organic material at an available adsorption site. The slowest step also known as the rate limiting step differs for physical and chemical adsorption. For physical adsorption the rate limiting step is one of the diffusion steps. For chemical adsorption, the rate limiting step is the adsorption step [11].

Both granular and powder activated carbon are capable of removing emerging contaminants via adsorption. Powder activated carbon has been found to achieve, in general, better results than granular activated carbon [14]. Powder activated carbon has achieved better results to granular activated carbon because of its greater surface area to volume ratio. Repeated use will reduce the activated carbons removal efficiency as

available surface sites for sorption become filled, and will require replacement or regeneration.

2.5.3 Direct Oxidation

Chemical oxidants are used during water treatment to control odor, control hydrogen sulfide, remove color, remove iron and manganese, disinfection, control biofilm growth and fouling, as well as oxidizing trace organic constituents including emerging contaminants. The most common oxidants used in water treatment include: ozone, hydrogen peroxide, permanganate, chlorine dioxide, and chlorine [11]. Chemical oxidants can produce more harmful byproducts than the constituents they target [11]. Their use in water treatment should be carefully monitored and limited to maximize efficiency and minimize potential toxicity [11].

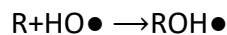
Ozone is an efficient method of disinfection and pollutant removal without a large production of disinfection byproducts. However, in special cases, like when bromide is present, disinfection byproducts can be formed during ozonation [15]. Some CECs are more reactive to oxidation by ozone alone, where others, also known as ozone recalcitrant, require additional treatment [15]. advanced oxidation processes (AOPs) might effectively treat ozone recalcitrant CECs.

2.6 Advanced Oxidation Processes

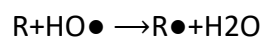
AOPs are processes that form hydroxyl radicals (\bullet OH), the most reactive oxidant. The most common AOPs on a commercial scale include ozone/UV, ozone/hydrogen peroxide, ozone/UV/hydrogen peroxide and UV/hydrogen peroxide [11]. AOPs are capable of

further treatment and destroying trace constituents following tertiary treatment. Some AOPs differ from typical oxidants because they do not present the potential formation of toxic byproducts [11]. In addition, they are capable of oxidizing compounds that conventional oxidants cannot. AOPs provide many benefits other forms of advanced treatment do not, including their ability to degrade constituents rather than concentrating them or transferring them into a different phase, as seen with physical treatment processes. In addition, AOPs can destroy compounds that cannot be adsorbed or are semi-adsorbable [11]. Due to the nature of AOPs, unlike many advanced processes, neither increased pressure nor increased temperature are necessary. In addition, AOPS are capable of chemically treating contaminants that are resistant to direct oxidation. AOPs are successful because of their ability to produce high levels of hydroxyl radicals. Hydroxyl radicals are a strong oxidant capable of complete oxidation of contaminants with no restriction to specific groups of compounds [11]. Hydroxyl radicals break down organics using different methods, as demonstrated in the reaction equations below: radical addition, hydrogen abstraction, electron transfer and radical combination.

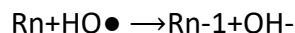
Radical Addition



Hydrogen Abstraction



Electron Transfer



Radical Combination



Radical addition of compounds with double bonds and hydrogen abstraction are the most common methods. In the context of wastewater treatment, hydroxyl radicals can be formed as a product of ozone and hydro-peroxides decomposition or UV-based treatment.

Current AOPs share various drawbacks including high cost of operation, production of hazardous oxidative byproducts in some cases, and variable removal efficiency [15]. Considering these shortcomings, it would be advantageous to develop new treatment technologies to optimize or replace current AOPs. One such alternative AOP currently under investigation is catalytic ozonation.

2.6.1 Carbon Nanotubes and Ozone

Catalytic ozonation is the process in which metal oxide or activated carbon surfaces promote the degradation of ozone into $\bullet OH$, resulting in higher $\bullet OH$ production than ozonation alone [15]. Activated carbon is an effective catalyst for $\bullet OH$ production; however, structural failings occur after repeated exposure to ozone [15]. Current studies suggest activated carbon is an effective catalyst because of its high surface area and basic surface functionalities.

Carbon nanotubes (CNTs) are cylindrical molecules formed by rolling up a single sheet or multiple sheets of graphene. CNTs share similar properties to activated carbon, however CNTs hold other features including high external surface area, tremendous mechanical strength and thermal stability [15]. When MWCNTs are exposed to ozone for extended periods of time, ozone promotes formation of active oxygen functional groups on the CNT surfaces. These functional groups are believed to further promote ozone breakdown into

- OH in solution.

Past research on MWCNTs and ozone as a form of water treatment has largely been performed as batch reactions [15], [29]. In these systems, MWCNTs have been suspended in the solution containing the CEC attempted to be removed. Ozone was added via aliquot (batch reactions) or bubbled into the solution (semi-batch reactions), and samples were taken from the system to determine contaminant removal [29]. The problem with MWCNTs in a batch system as described is the lack of full scale feasibility and potential risk to the environment. MWCNTs are a current concern because of the unknown environmental and human health risks that they may pose. By its very nature performing a batch reaction with freely suspended MWCNTs allows for potential loss of MWCNTs or MWCNT products during treatment. Before a full scale CNT system could be implemented in a treatment facility, the technology would need to guarantee no CNT leaching into the effluent water. A constant flow system, with a CNT enabled membrane may be a more viable choice for a full scale set-up and better contain CNTs from accidental environmental exposure.

2.7 Nano-Enabled Material

CNT membranes are a new technology, created less than 20 years ago, that describe membranes enhanced with CNTs or fabricated out of CNTs [17]. CNT membranes can be distinguished by three different fabrication techniques. The first and more complicated fabrication method aligns the CNTs vertically. The vertical alignment allows the membrane to achieve a relatively high water flux. The second fabrication technique mixes CNTs with a polymer and layered it on a fabric, very similar to how a reverse osmosis membrane is fabricated. The third method, called the Bucky paper method is fabricated by vacuum filtering MWCNTs dispersed in solution onto a flat sheet membrane [17].

The vertical alignment method achieves the best flux however it requires a special operating system and the membranes themselves are difficult to construct. The polymer method and Bucky method achieve similar fluxes and can both be used in simple systems. [17]

2.7.1 Practical Applications

For MWCNTs coupled with ozone to be a realistic AOP in the field, treatment must evolve from a batch reactor system. MWCNT-enabled membranes are a plausible solution to the batch treatment problem. By using a membrane, MWCNTs will be contained during treatment, while still maintaining sufficient exposure to contaminated water. Lab tests performed by Dr. Rebekah Oulton, Stephen Penrose, and Emily Miller found the “Bucky Method” (refer to Methods section) to produce the best results in the lab as a MWCNT enabled membrane [15]. One theoretical application of the membrane produced from

the Bucky Method can be seen below in Figure 3. The schematic illustrates influent water being ozonated and pumped to two separate MWCNT enabled membranes.

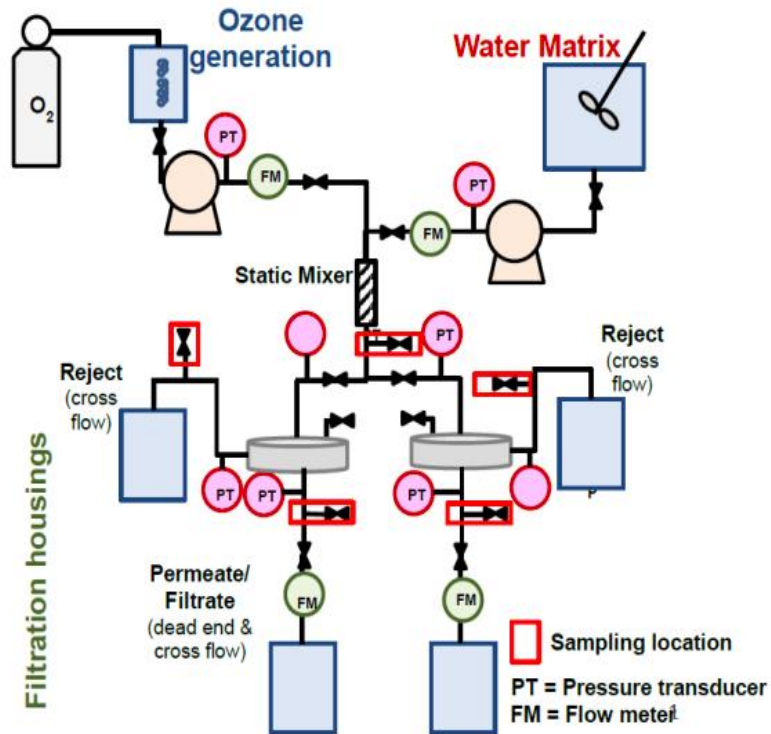


Figure 3: Schematic of Flow-through system. Schematic created by Jason Haas, Adopted from Oulton. [15]

2.8 Fourier Transform Infrared Spectroscopy

Fourier Transform Infrared (FTIR) Spectroscopy studies absorbance and emission of infrared radiation by matter. As infrared radiation is passed through a sample, some is absorbed and some is transmitted. The result is a spectrum representing a molecular “fingerprint” of the sample. (Figure 4)

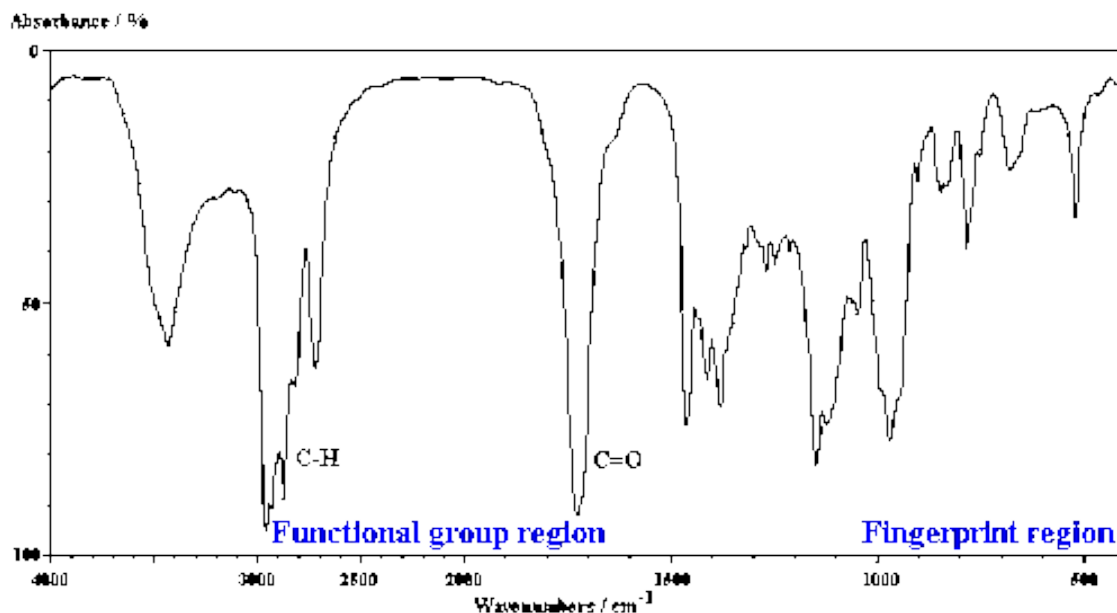


Figure 4: FTIR example spectra. [18]

FTIR Spectroscopy can be used to identify and characterize chemical structures. Attenuated Total Reflectance (ATR) FTIR Spectroscopy is a technique used to measure the infrared spectra of solids and liquids as well as “probing adsorption on particle surfaces” [19]. ATR works by measuring the changes that occur in a reflected infrared beam when the beam contacts a sample. After the beam contacts the sample, the transmitted beam returns to a crystal in the ATR accessory. This internal reflectance creates an evanescent wave that extends from the surface of the crystal to the sample and the detector in the spectrometer [20] (Figure 5).

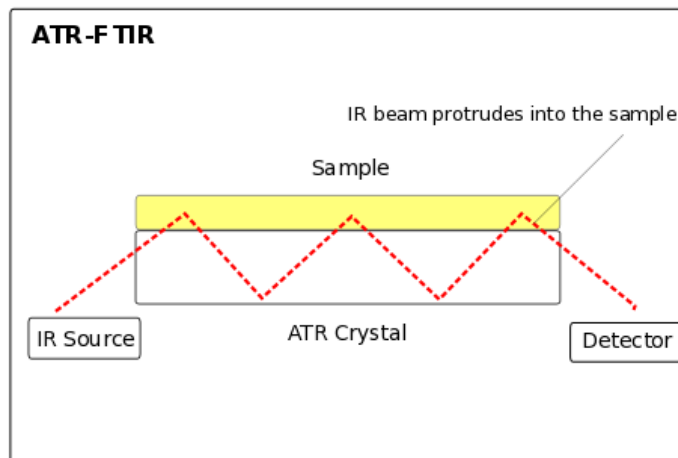


Figure 5: FTIR-ATR figure depicting reflectance off a sample [21].

The FTIR Spectrometer generates spectra graphs with patterns that can be identified as specific functional groups. (Figure 6) One of the main drawbacks of FTIR Spectroscopy is that, although it can identify existing functional groups, it cannot determine the number or concentration of functional groups present.

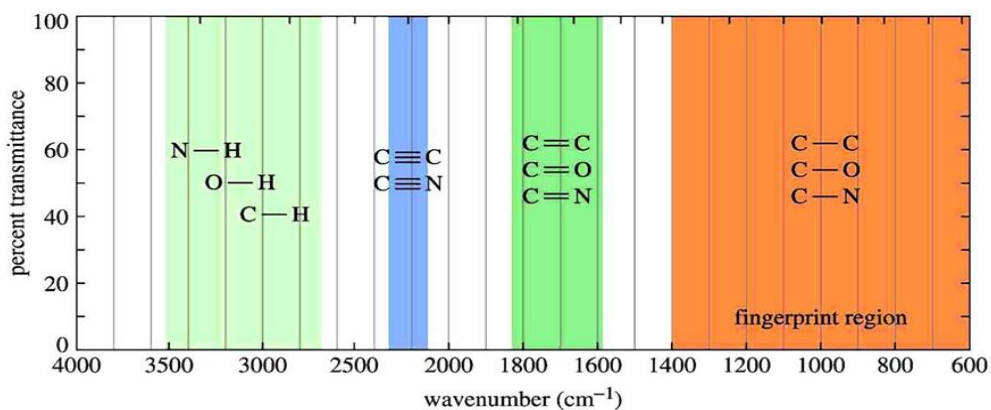


Figure 6: Spectra labeling common functional groups [22].

2.9 Fourier Transform Infrared Spectroscopy Results for CNTs

FTIR has had varying levels of success when used to analyze functionalized CNTs. A more promising study conducted by Sahebian, S. et al. compared pure MWCNTs with MWCNTs

functionalized with 50 mL of concentrated HNO₃ for durations of 1, 2 and 4 hours [23]. The samples were analyzed using a transmission electron microscope (TEM), FTIR, UV-Vis, as well as Raman Spectra. The FTIR spectra for the pure sample (P-MWCNT), 1, 2 and 4 hour functionalized samples (F-MWCNT-1 h, F-MWCNT-2 h, F-MWCNT-4 h) are displayed in Figure 7 [23].

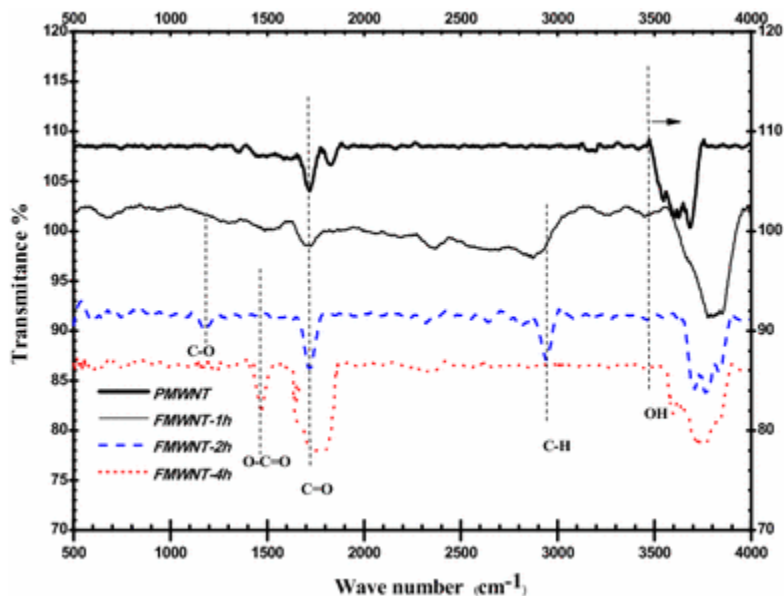


Figure 7: Functionalized samples, FTIR spectra of P-MWNT, F-MWNT-1 h, F-MWNT-2 h, and F-MWNT-4 h, FTIR spectra [23].

Low intensity spots at around 3440 and 1711 nm correspond to functional groups • OH and C=O. Water observed on the surface of the CNTs likely relates to the • OH peak. The functionalized samples contain an additional peak around 1719 nm caused by C=O stretching, indicative of a carboxylic group created during oxidation. The intensity of the C=O peak implies a greater presence of the carboxylic groups. In addition, the F-MWCNT-2 h sample contained peaks at 2923 and 2853, representative of a CH₂ group. This study

found that “when the time of acid treatment increases, the intensity of hydroxyl and carboxyl groups in spectrum goes toward a high value” [23]. Given this study, it is expected that with extended ozone exposure hydroxyl and carboxyl groups will be visibly present in high values on the FTIR spectra.

In a separate study, six commonly used oxidants were used on MWCNTs and compared using X-ray photoelectron spectroscopy, energy dispersive spectroscopy and FTIR [24]. FTIR could not discern any “spectral features.” The study proposed sources of error including percent surface loading and likelihood of water present on the exterior surface of the CNTs. Vibrational intensity present at 3200 cm^{-1} is often “swiftly” assigned to hydroxyl groups rather than water that might be present on the exterior [24]. This study finds FTIR to not be an effective technique for identifying functional groups on the surface of MWCNTs. This study suggests that FTIR may not be feasible when MWCNT surface loading is $>5\%$ [24].

2.10 Electron Microscopy

The scanning electron microscope (SEM) is unique compared to other microscopes because instead of using light to outline and formulate images it uses electrons. Samples are scanned in a vacuum or vacuum like environment using a focused electron beam. The focused electron beam interacts with the surface of the sample, producing signals composed of “secondary electrons, backscattered electrons and characteristic x-rays” representing the surface topography and composition [25]. The image produced is 3-D and black and white composed on a computer screen.

Transmission electron microscopy (TEM) is another form of electron microscope that passes electrons through the sample it is taking an image of. Unlike SEM, TEM is able to give details about internal structures. TEM is a less universal form of electron microscopy because it requires the samples be thin enough to pass electrons through.

2.11 SEM & TEM Results for CNTs

Exposure to oxidants can cause changes to the surface of MWCNTs resulting in variations in size, porosity, length, and curvature. Imaging using an electron microscope can help show both changes to the CNTs themselves as well as changes to the membrane's surface. One study compares the qualitative properties of MWCNTs following oxidation using various oxidants. Figure 8 shows SEM microphotographs of both pristine (P) and functionalized (f) MWCNTs. Following oxidation, smaller aggregates and tangled clusters are present in all samples. In addition, MWCNT length is notably shorter following oxidation [26].

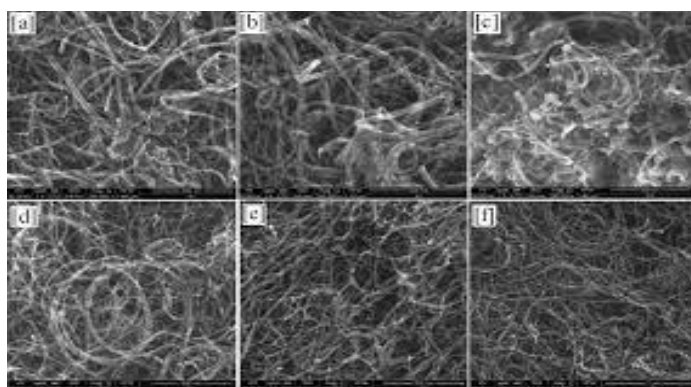


Figure 8: SEM of MWCNTs: (a) pristine A-type MWCNTs, (b) A-type f-MWCNTs (HNO_3), (c) A-type fMWCNTs ($NH_4OH + H_2O_2$), (d) pristine P-type MWCNTs, (e) P-type f-MWCNTs (HNO_3), (f) P-type fMWCNTs ($NH_4OH + H_2O_2$) [26].

SEM is valuable for looking at large groups of CNTs; to further investigate the quality of the surface on specific CNTs, TEM is a better fit. TEM is capable of producing images of such magnification that diameter, number of walls, presence of adsorbed amorphous carbon, and concentration of defect sites on the side-walls of CNTs can be seen [24]. Similar to the Figure 8 above, the following figure shows TEM images of MWCNTs after exposure to various oxidants. (Figure 9)

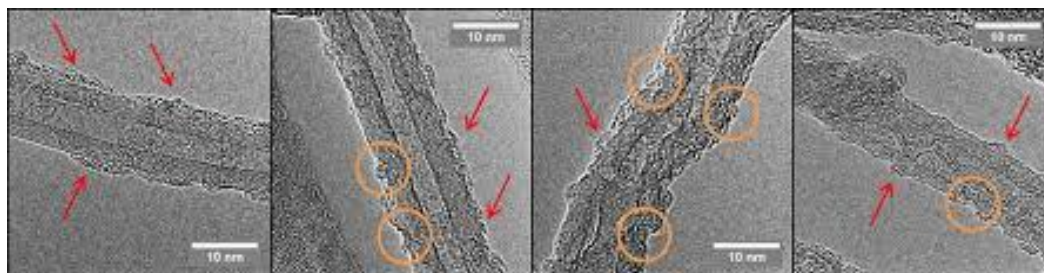


Figure 9: Representative TEM Micrographs (left to right): pristine MWCNTs (0.9% O), H₂O₂ treated MWCNTs (4.5% O), H₂SO₄/HNO₃ treated MWCNTs (5.1% O), KMnO₄ treated MWCNTs (5.3% O). Amorphous carbon is indicated with arrows, sidewall defects highlighted by circles [24].

TEM images show the presence of free reactive carbon, otherwise known as amorphous carbon, around the pristine MWCNTs. In addition, the pristine MWCNTs appear long and straight with uniform and primarily defect-free sidewalls. H₂O₂- and KMnO₄-treated MWCNTs showed few defect sites on the outermost sidewall of the MWCNTs as well as reduced presence of amorphous carbon. HNO₃- and H₂SO₄-treated MWCNTs experienced extreme structural damage with defects reaching past the outermost wall as well as a change in general linearity [24].

2.12 UV-Vis Spectroscopy

UV-Vis Spectroscopy (UV-Vis) is a quantitative technique that measures the intensity of light passing through a sample compared to the intensity of light passing through a reference blank. It provides a measurement of adsorption/transmission vs wavelength. This technique can be used on solid and liquid samples. UV-Vis can be used to determine the concentration of a specific substance. The Lambert-Beer Law states that the higher the absorbance at a specific wavelength, the higher concentration of a known substance [27]. The Lambert-Beer Law equation calculates absorbance (A) given absorptivity at a specific wavelength (ϵ_{λ}), concentration (c) and optical path length (b). (Equation 1)

$$A = \epsilon_{\lambda} * c * b \quad \text{(Equation 1)}$$

2.12.1 UV-Vis Results for CNTs

In the study conducted by Sahebian, P-MWCNTs and F-MWCNTs-2 h were sonicated for 5 minutes and left to stand for half an hour and 20 days. The samples were then measured using UV-Vis, across a UV-Vis spectrum of 190 to 800 nm. The P-MWCNT sample achieved maximum absorbance around 209.5 nm, a wavelength associated with the C–C aromatic bond of CNT structure” [23]. Comparing the 30-minute sample to the 20-day sample showed that the absorbance value decreased with time. This result indicates the hydrophobic behavior and low dispersion of non-functionalized MWCNTs in water. Sample F-MWCNT-2h achieved maximum absorbance around 209.5, indicative of the C-C bond, and also a second peak at 293.5 nm indicating the C=O bond expected with functionalization. The absorbance for the functionalized MWCNTs is significantly higher than that of the non-functionalized MWCNTs and is consistent across the two delay

periods. The formation of carboxyl and hydroxyl groups on the surface of the MWCNTs improves hydrophobicity and consequently improves solution stability [23].

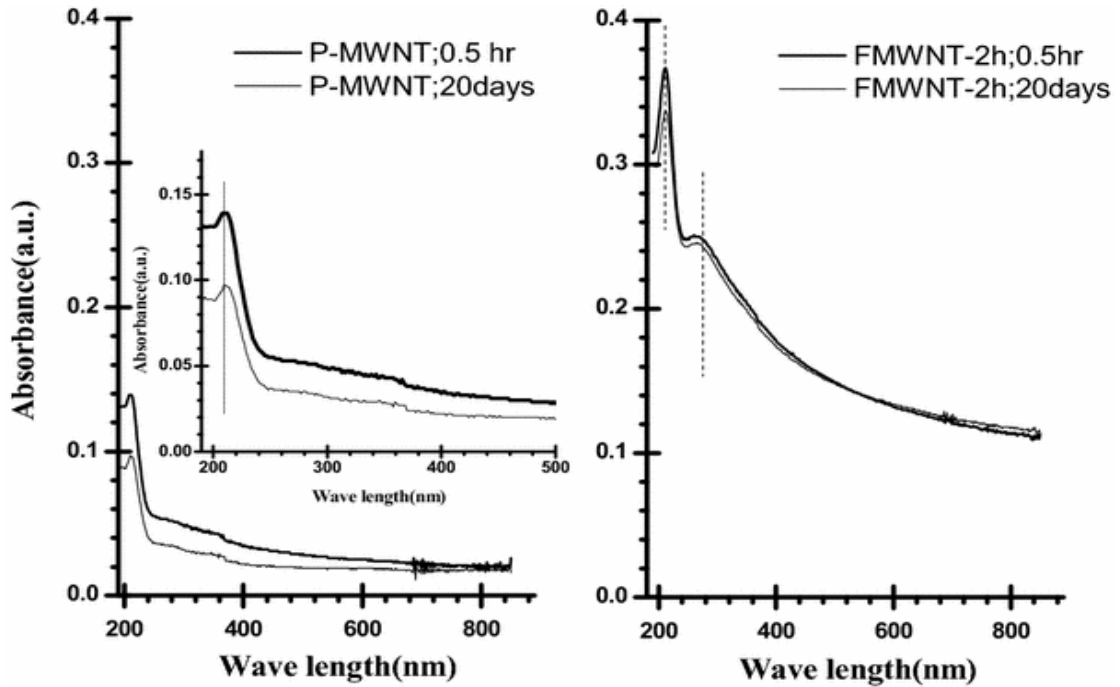


Figure 10: The UV-Vis spectrum of P-MWNTs and F-MWNT-2 h in water after half an hour and 20 days of 5 min ultrasonic mixing [23]

3. METHODS

New AOPs are required to target ozone recalcitrant CECs, like Atrazine. Ozonated MWCNTs show promise as a method of treatment but require a fabrication method capable of retaining the MWCNTs. MWCNT enabled membranes are one solution however their removal efficiency and longevity are still unknown. Ozone is a strong oxidant that may change the surface chemistry and strength of MWCNTs over extended exposure. Analytical techniques including FTIR, SEM and UV-Vis may provide insight into these chemistry and surface integrity changes, and thus the longevity of MWCNT enabled membranes.

3.1 CNT Functionalization Procedure

Following a procedure developed by others, a solution of 40 mg CNTs (NanoLabs) in 100 ml 70% nitric acid was sonicated in a Branson 2800 Sonicator for 1 hour [15]. After sonication, the solution was refluxed at 140 degrees Celsius for 1.5 hours, from the start of boiling. Afterwards, the solution was allowed to cool to room temperature overnight. A vacuum filtration system, equipped with a 47-mm nylon membrane, was used to filter the CNT solution with DI water until the effluent solution reached pH greater than 5. The CNT embedded membrane was completely dried overnight in an oven with $T > 100^{\circ}\text{C}$. Using a metal spatula, dried CNTs were removed from the membrane and pulverized into a fine powder using a ball mill. CNTs were then mixed with DI to form a 1 g/L solution and sonicated for at least 20 hours. Prior to subsequent uses, this CNT solution was re-sonicated for at least 30 minutes [15].

3.2 Bucky Method

What will be referred to as the “Bucky Method” is a technique to prepare CNT-enabled membranes [17]. A 47-mm nylon membrane was restricted in a vacuum functioned filtration system. To pre-rinse, approximately 25 mL of deionized (DI) water was filtered through the membrane. 15 mL of DI water followed by 3.47 mL of 1 g/L CNT solution was measured into the vacuum filtration funnel. The resulting solution had a solid loading of 0.2 mg CNTs/ cm² membrane. The vacuum pump was powered on, and kept running, until solution had passed completely indicating CNTs had been embedded. Using a flat edge tweezer, the membrane was removed and placed faceup in a petri-dish. The membrane was left to dry at room temperature for a minimum of 18 hours before use [15].

3.3 CNT Membrane Lab Testing Procedure

3.3.1 Atrazine Solution

A 1 g/L Atrazine (Chem Services) solution was prepared using HPLC-grade methanol due to Atrazine’s hydrophobic nature.

3.3.2 Phosphate Buffer

A 680 mg/L phosphate buffer solution was prepared using DI water and potassium phosphate monobasic (Fischer Scientific). The phosphate buffer solution was adjusted to 7.0 pH. Afterwards, the phosphate buffer solution was bubbled with ozone using a ClearWater Tech LLC CD1500P ozone generator fed with oxygen gas for approximately 20 minutes, to remove any ozone-reactive compounds that might be present in the buffer

solution prior to use. The phosphate buffer solution was deoxygenated for several hours prior to use.

3.3.3 Sodium Sulfite Solution

Sodium sulfite serves as an ozone quencher. A sodium sulfite solution was prepared to ensure the reaction in each sample was terminated prior to analysis. A 50 mg/L sodium sulfite solution was made in 25 mL of DI water. Due to potential for reaction with air, the solution was prepared daily prior to each experiment and kept sealed in between uses [15]. 25 μ L of Sodium Sulfite was used in the sample collection vials to immediately quench the reaction upon collection of the sample, and 2.5mL was used in the collection flask of the vacuum apparatus during experimental runs.

3.3.4 Ozone

For testing, 93 mL of the prepared phosphate buffer solution was measured into a 200mL Erlenmeyer flask. Prior to use the Erlenmeyer flask was filled with glass beads and stored in a freezer to promote a cold environment. The Erlenmeyer flask with the phosphate buffer solution was placed in an ice bath and bubbled with ozone using a ClearWater Tech LLC. Ozone Generator (CD1500P) for approximately 30 minutes, or until dissolved ozone absorbance stabilized around 0.8-1.2 A. The dissolved ozone absorbance was measured using a Thermo Scientific Genysys 10S UV-Spectrometer ($\epsilon_{258} = 2,900 \text{ M}^{-1}\text{cm}^{-1}$) [15]. The constant concentration calculated using Beer's Law was within 190 μ M and 330 μ M for all experiments. Once a steady absorbance was achieved, the solution was transferred from the Erlenmeyer flask to the upper portion of the vacuum filter apparatus. The phosphate buffer solution was ozonated in the apparatus for an additional 5 minutes, and

the final stable ozone absorbance was measured. Note that ozone bubbling continued throughout the experiment. For each experimental run, this final stable ozone concentration was assumed to be maintained throughout the duration of the experiment [15].

3.3.5 Vacuum Filter Process

The beaker containing 0.5 mL Atrazine and 13 mL tert-butanol was poured into the ozonated phosphate buffer solution in the vacuum filter apparatus (Figure 11). Two initial samples were taken before powering the vacuum pump. A timer was set to measure the time required for the solution to completely filter to the collection flask of the vacuum apparatus. Two final samples were taken from the collection flask. All four samples were filtered through 2 um filters to remove any CNTS that may have detached from the CNT membrane [15]. After filtration, samples were transferred to HPLC vials and labelled appropriately with date and description of sample. Note: Beginning January 13th temperature and relative humidity measurements were recorded during testing as well [15].



Figure 11: Vacuum filtration process under fume hood.

3.3.6 Analysis for CNT Membrane Lab Testing

Samples were analyzed using Thermo Scientific UltiMate 3000 Ultra High Performance Liquid Chromatography (HPLC) system with an Acclaim 120 C18 column (4.6x 100 mm, 5 μ m internal diameter). An eluent solution of 60% acetonitrile and 40% DI water was used, with an injection volume of 1 μ L and a flow rate of 1 mL/min. The absorbance was measured at 226 nm [15].

3.3.7 Quality Assurance and Analysis of Filtration and HPLC Procedure

A calibration curve for Atrazine was created with samples ranging from 0.1 μ M to 10 μ M. This was repeated periodically throughout experimental trials.

As a daily control, an un-ozonated sample was run through a blank membrane and a functionalized MWCNT membrane to ensure sorption was not occurring. Lastly, duplicate samples were taken to assure consistency.

3.4 FTIR Procedure

Samples were analyzed using JASCO FT/IR-4600 with ATR accessory. For a full description of the FTIR procedure refer to the appendix a. Before testing samples, the sample tray was rinsed with isopropyl alcohol and dried with chem-wipe. The membrane was placed CNT side down onto the sample tray. The mount was aligned and lowered using the hand knob until gently applying pressure on the sample. The spectrometer software was used to produce an image of absorbance with respect to wavenumber. Once the image was saved, the membrane was removed and the mount was cleaned with isopropyl alcohol.

3.4.1 Quality Assurance and Analysis of FTIR Procedure

Blanks were performed after starting the program and turning on the machine to confirm proper calibration. A blank membrane was used as a control to determine efficacy of spectra. Measurements were taken in triplicate for each sample, producing three spectra for each membrane. Measurements were taken in triplicate on different spots of the membrane to determine outlier peaks, as well as general trends for the surface of the membrane.

3.5 Scanning Electron Microscope Procedure

Samples were viewed using a FEI Quanta 200 Environmental Scanning Electron Microscope (ESEM) with an Everhart-Thornley Detector. Chosen membranes were carefully cut into 0.75 cm by 0.75 cm squares. Due to the nature of the SEM procedure samples chosen to be viewed can no longer be used for future filtration, i.e. lab testing. Membranes were mounted onto 12 mm aluminum stubs using double sided graphite tape

(Figure 12). ESEM was run at High Vacuum Mode. The spot size was set at 1.5, with a working distance of 7.0mm. The acceleration voltage was set at 30,000V. Samples were viewed using a slow scan speed with image integration.

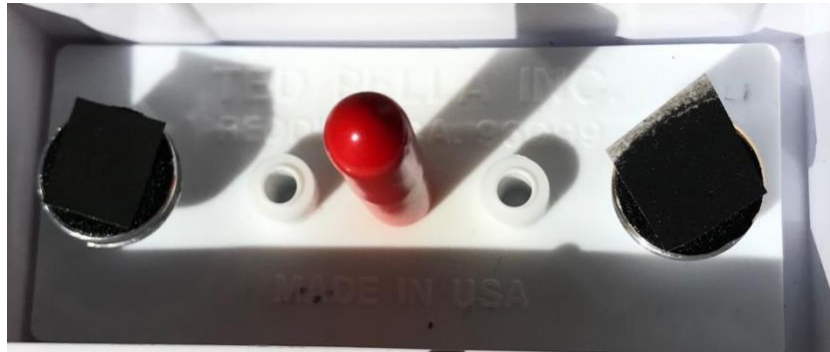


Figure 12: Membrane 3B (on left) and Membrane 5 adhered to 12 mm aluminum stubs.

3.5.1 Quality Assurance and Analysis of SEM Procedure

Ideal conditions for using the SEM must be met prior to testing. These conditions include an ambient temperature below 68 degrees Fahrenheit and a relative humidity below 20%. Membrane samples were left to dry in a fume hood for 24 hours prior to imaging to prevent damage of the instrument or reduced image quality. When choosing ideal sample areas on the membrane, spots were chosen with no visible holes, foreign objects, or discoloration. Five images were taken for each membrane, excluding membrane 2B due to technical difficulties. Each image was taken of a different area on the membrane to provide a more inclusive representation of the membranes surface.

3.6 UV- Vis Procedure

A 1 g/L CNT solution was sonicated for 30 minutes. Next, 15 mL of DI water followed by 3.47 mL of 1 g/L CNT solution was measured into a sealable glass bottle. The glass vial was sonicated for 5 minutes. Using a pipet, the MWCNT solution was transferred into a cuvette. Using Thermo Scientific Genysys 10S UV-Spectrometer, absorbance measurements were taken every 0.2 nm from 190-745 nm [23].

3.6.1 Quality Assurance and Analysis of UV-Vis Procedure

Measurements were taken in triplicate to identify any outliers and to observe probable peaks.

4. RESULTS AND DISCUSSION

The goal of experimentation was to collect sufficient data so that comparisons could be made between different membranes regarding efficacy of pollutant removal and continued efficacy over repeated uses.

4.1 Percent Removal

Percent removal was found by measuring the concentration of Atrazine in the influent solution and effluent solution using a HPLC. Environmental and operational factors were tracked to determine what effect they might have on removal for the target contaminant. These factors included: percent relative humidity, ambient temperature, filtration time, ozone absorbance, ozone exposure, number of samples filtered and percent removal of the target constituent were measured.

Note that membrane 6 experienced three unusual runs. Runs 4, 7 and 9 accomplished either negative percent removal which is impossible or unrealistically high percent removal. For the sake of discussion membrane 6 has not been included in discussion figures. To see graphs that contain membrane 6 please refer to the appendix.

4.1.1 Relative humidity and ambient temperature

Percent relative humidity and ambient temperature were recorded after the fact using historical data for the date testing was performed. Tests were performed between September 2019 and March 2020. Ambient temperature in the lab ranged from 52 degrees Fahrenheit to 83 degrees Fahrenheit. Similarly, percent humidity held a broad range from 25% to 83%. Temperature and relative humidity are important factors to

ozone concentration for two main reasons. Lower temperatures improve dissolution of ozone in water [15]. In addition, relative humidity has been found to deplete ozone in air which would suggest ozone dissolution in water.

Percent humidity and temperature seem to have no effect on either ozone absorbance (which correlates to ozone concentration) (Figures 13 & 14) or percent removal of the contaminant (Figures 15 & 16). Due to the nature of testing, humidity and temperature of the experimental system were relatively controlled using a fume hood and ice bath. The results are representative of lab testing with a controlled environment which is not an accurate representation of what a similar system would experience in the field.

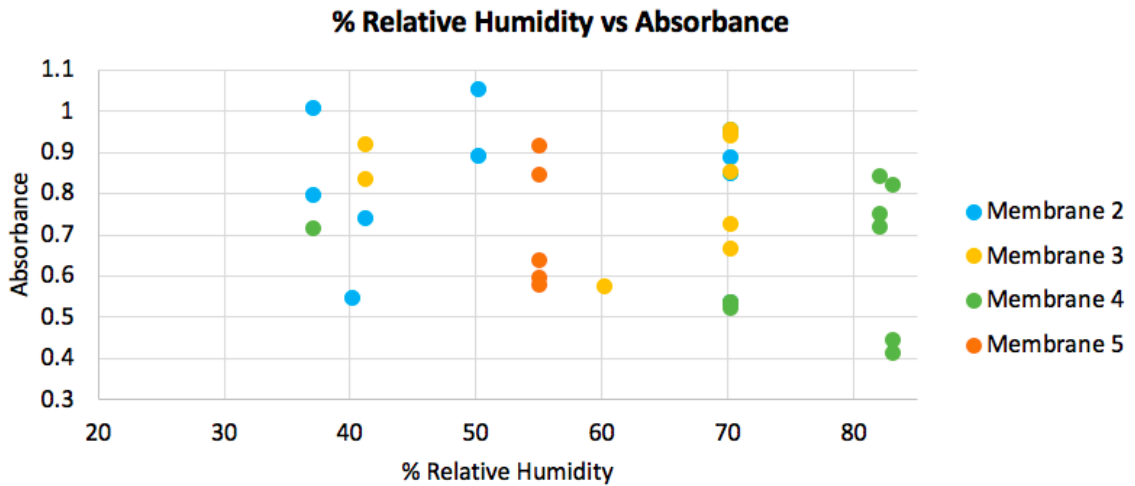


Figure 13: Percent relative humidity compared to ozone absorbance.

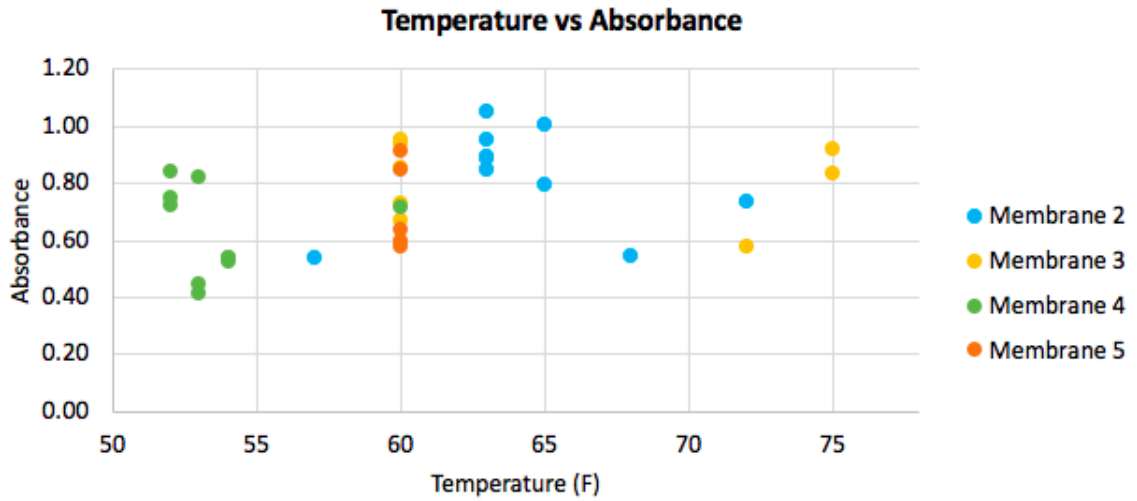


Figure 14: Ambient temperature compared to ozone absorbance.

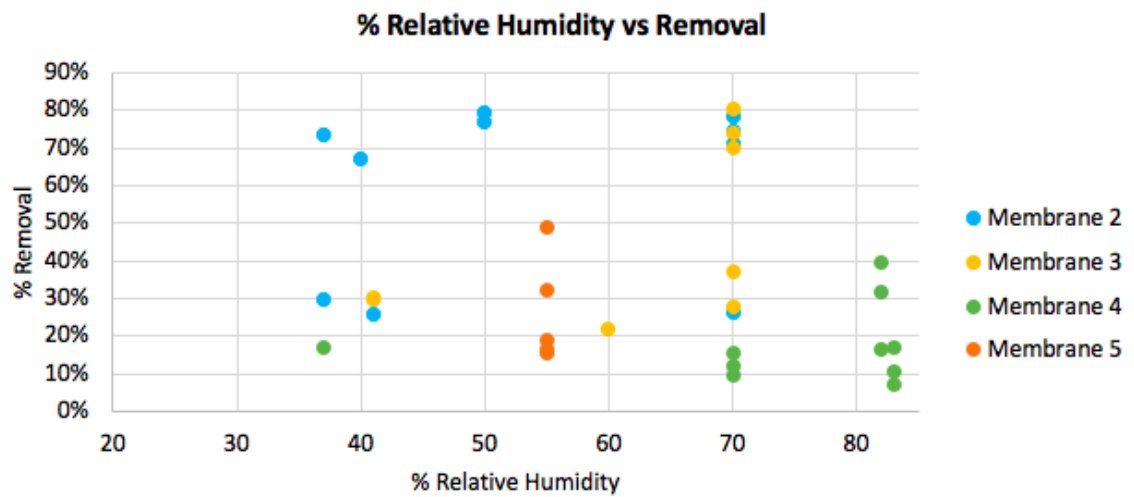


Figure 15: Relative humidity compared to percent contaminant removal.

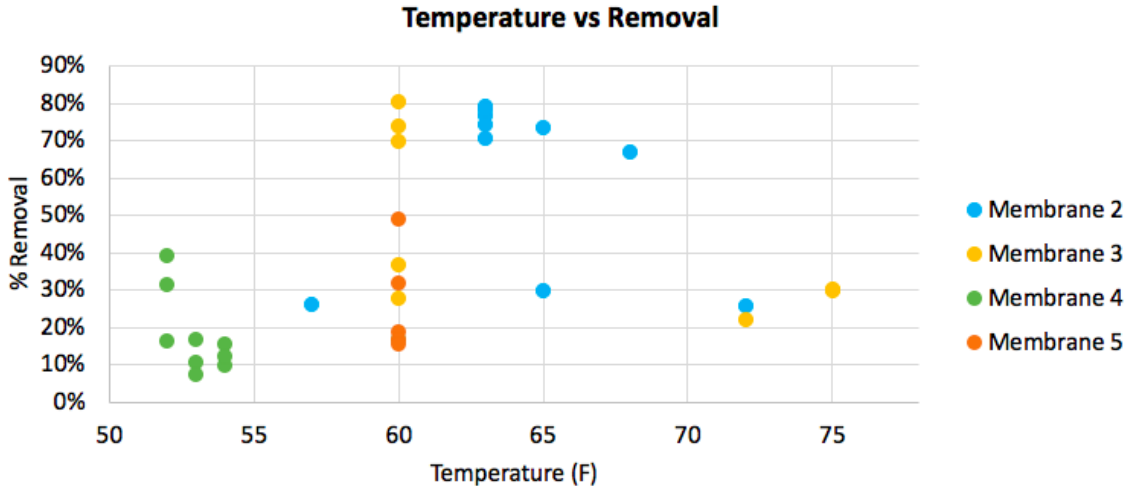


Figure 16: Ambient temperature compared to percent contaminant removal.

4.1.2 Filtration Time

Filtration time was measured in minutes from when Atrazine was added and the vacuum process began until no liquid was observed on the surface of the membrane. Different membranes required different lengths of time to complete filtration, ranging from under 5 minutes to nearly an hour (Figure 16). Percent removal tended to increase with filtration time. Membranes 2 and 3 required the longest filtration time and achieved a high percent removal. In contrast, membranes 4 and 5 had the lowest filtration time and achieved the lowest percent removal. The coefficient of determination (R^2) was roughly 43%.

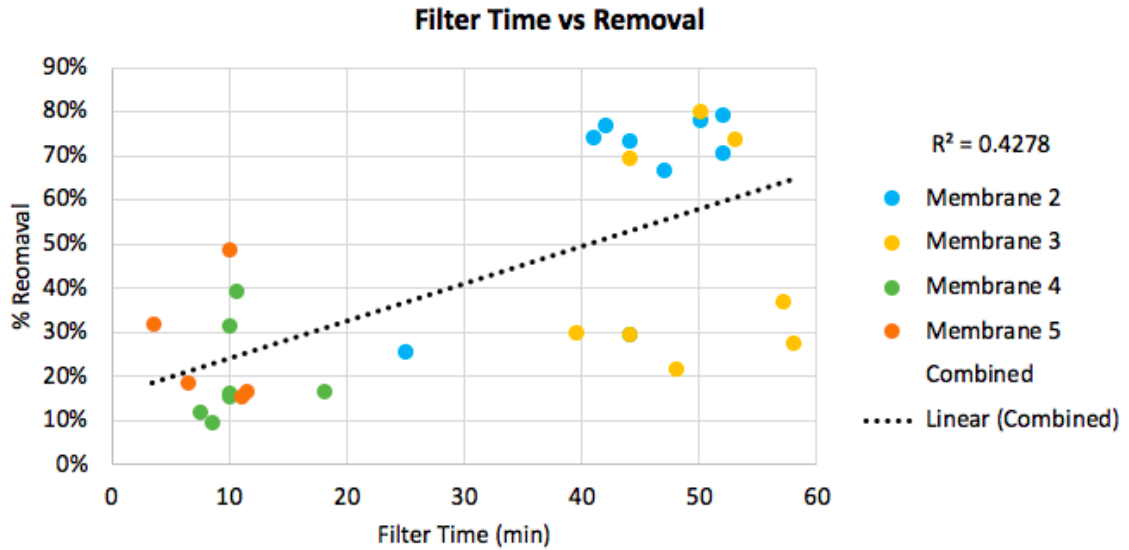


Figure 17: Filtration time compared to percent contaminant removal.

4.1.3 Steady-State Ozone Concentration

As discussed above, ozone absorbance measured immediately before filtration was assumed to be indicative of steady-state ozone concentration during filtration. There appears to be a slight trend between ozone absorbance and percent removal, though the R^2 value of 0.310 indicates this trend is not significant (Figure 18).

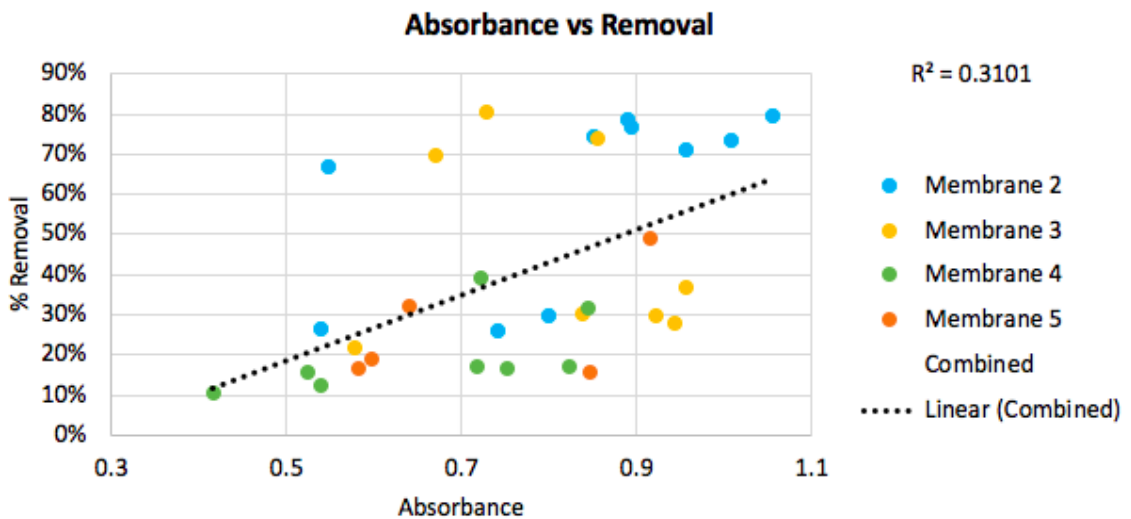


Figure 18: Ozone absorbance in solution compared to percent contaminant removal.

4.1.4 Ozone Exposure

Due to the apparent trend between percent removal and filtration time, and possible relationship between percent removal and ozone concentration during filtration, a correlation between ozone exposure and percent removal was also examined. Ozone exposure is a value used in ozone chemistry studies to indicate the total amount of ozone available for utilization during a reaction. In this case, since ozone concentration was held constant, ozone exposure was determined using the measured ozone absorbance and filtration time. (Equation 2)

$$\text{Ozone Exposure} = [O_3] \int_0^t dt \quad (\text{Equation 2})$$

Recall that the solution is actually exposed to ozone for 10-15 minutes prior to filtration to achieve steady-state, transferred to the filtration apparatus prepared with the membrane and further ozonated until the ozone concentration returned to steady-state, before filtration was initiated. Exposure to ozone prior to filtration could not be found and is recommended as a variable to be measured in future testing. This method assumes that the majority of contaminant removal occurred during passage through the CNT-enabled membrane, where exposure to •OH would be the greatest, rather than during the ozonation process itself. Solutions filtered by membranes 2 and 3 had higher ozone exposure and achieved greater percent removal (Figure 19). The R² value for the trend between ozone exposure and percent removal is approximately 42%.

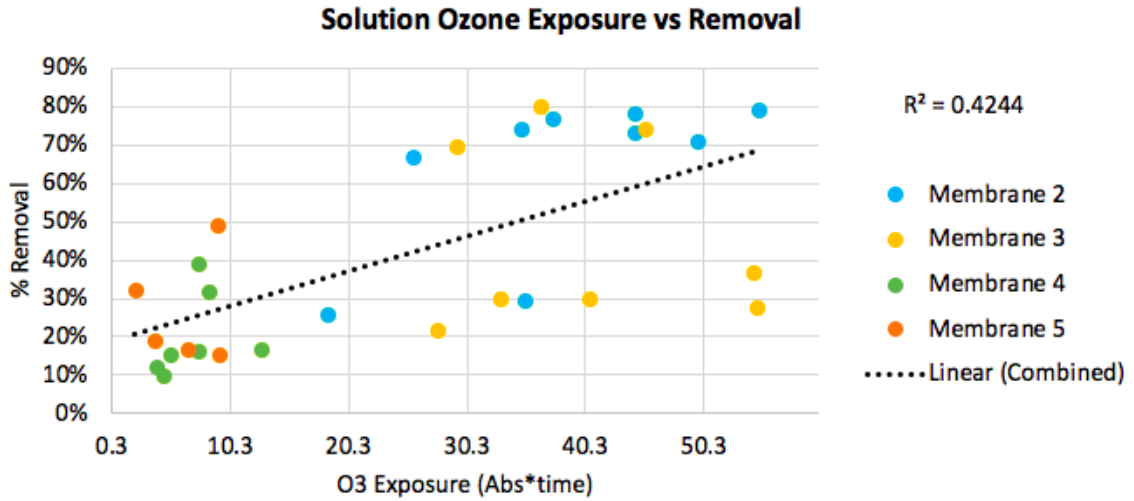


Figure 19: Ozone exposure in solution compared to percent contaminant removal.

4.1.5 Repeated Uses of Filter

Between 5-10 runs were performed on each membrane. The goal of running multiple runs was to determine if performance changed between runs. Figure 20, illustrating percent removal in terms of number of samples filtered, shows improved removal for all filters between run number two and three and a decrease in removal for three filters between runs nine and ten. There are no significant trends between one to ten runs; more runs should be considered for future testing.

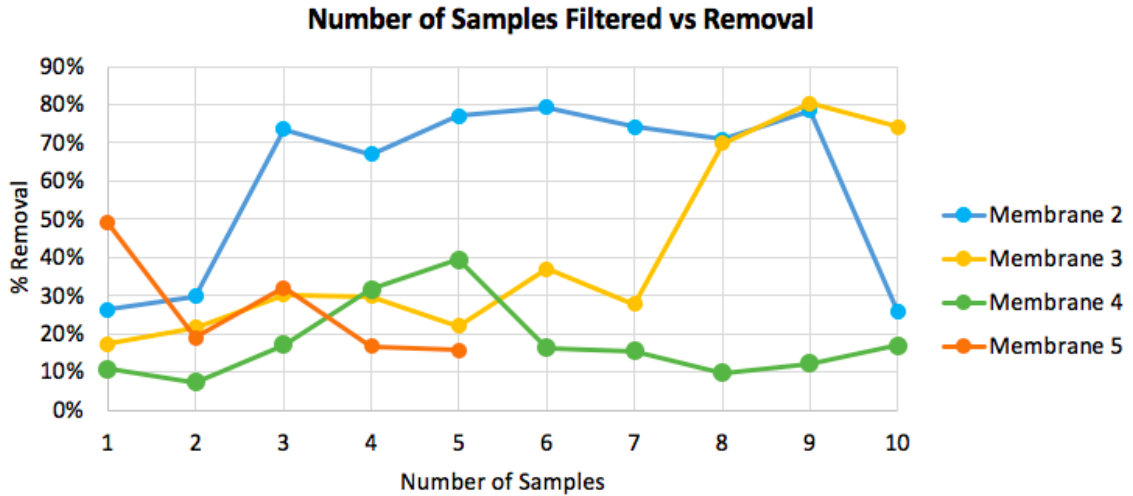


Figure 20: Number of samples filtered compared to percent contaminant removal.

4.1.6 Total Ozone Exposure

Similarly, ozone exposure for the membrane over the course of its life was calculated. Since ozone itself is an oxidant, extended exposure to ozone may change the surface chemistry of the CNTs, or the surface integrity of the membranes. Total ozone exposure was found for each membrane to determine if this extended oxidation may affect the efficacy of contaminant removal over continued use of the same membrane. (Figure 21)

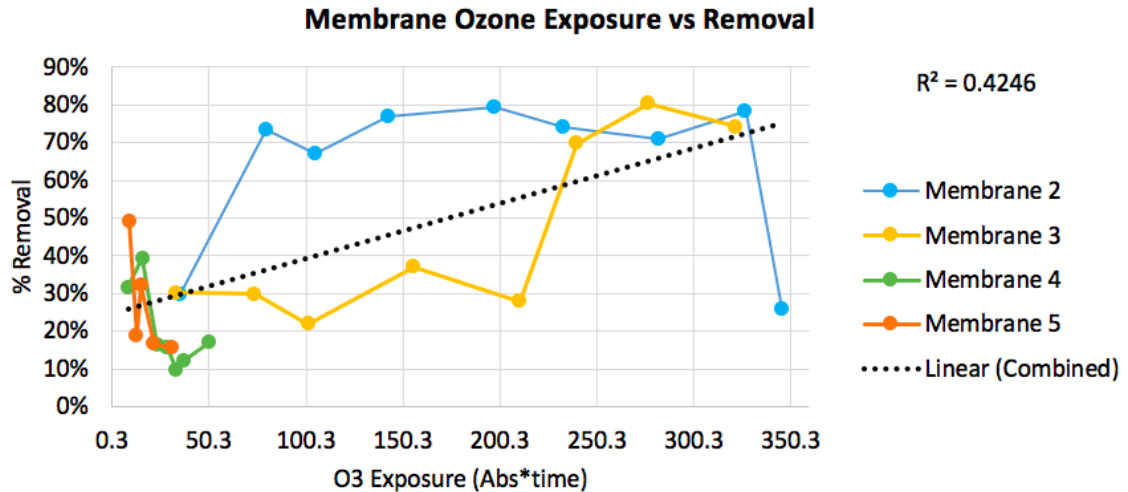


Figure 21: Ozone exposure over the life of the membrane compared to percent contaminant removal.

Membrane 2 experienced a sharp drop in percent removal when total ozone exposure reached 345 A * min. No other membrane reached this level of exposure so it is not possible to determine whether membrane 2 had exceeded its life or if this result was an anomaly. The R² value for the trend between ozone exposure and percent removal over the lifetime of the membrane is approximately 43%.

Figure 22 is a compilation of the three variables; solution ozone exposure, filtration time, and number of samples filtered on the horizontal axis and percent contaminant removal on the vertical access. Individual membrane responses are color-coded on the left hand graph, and results are graded to indicate magnitude. The larger the value, the darker the shading; the smaller the value, the lighter the color. Using this color-scheme, it is possible to see if trends exist for multiple variables with respect to percent removal. Figure 22 illustrates a general trend of higher ozone exposure and longer filtration time generally correlates with higher percent removal. Furthermore, it shows greater percent removal

by membranes 2 and 3. Membranes 4 and 5 had a wide distribution from the top to bottom of the figure.

Percent Removal	Membrane 2			Membrane 3			Membrane 4			Membrane 5		
	# of Samples Filtered	O3 Exposure	Time (min)	# of Samples Filtered	O3 Exposure	Time (min)	# of Samples Filtered	O3 Exposure	Time (min)	# of Samples Filtered	O3 Exposure	Time (min)
80%	9	36.5	50									
79%	6	54.9	52									
79%	9	44.5	50									
77%	5	37.5	42									
74%	7	34.9	41									
74%	10	45.4	53									
74%	3	44.4	44									
71%	8	49.8	52									
70%	8	29.5	44									
67%	4	25.8	47									
49%	1	9.2	10									
39%	5	7.6	10.5									
37%	6	54.5	57									
32%	3	2.2	3.5									
32%	4	8.5	10									
30%	3	33.1	39.5									
30%	4	40.6	44									
30%	2	35.2	44									
28%	7	54.7	58									
26%	1											
26%	10	18.5	25									
22%	2											
22%	5	27.8	48									
19%	2	3.9	6.5									
17%	1											
17%	10	12.9	18									
17%	3											
17%	4	6.7	11.5									
16%	6	7.5	10									
16%	7	5.3	10									
16%	5	9.3	11									
12%	9	4.1	7.5									
11%	1											
10%	8	4.6	8.5									
7%	2											

Figure 22: Compilation of notable results from filtration tests.

4.2 Membrane Longevity

Membrane longevity refers to the length of time or number of passes a membrane can be effective at providing contaminant reduction. In a full-scale application, membrane longevity would relate to the total volume of water able to pass through that membrane before treatment starts to decline. Results from testing found no significant change in filter time as a result of number of samples filtered. This result suggests that membrane longevity exceeds ten runs in a lab setting (Figure 23). Results suggest the membrane surface is not developing preferential pathways through repeated use.

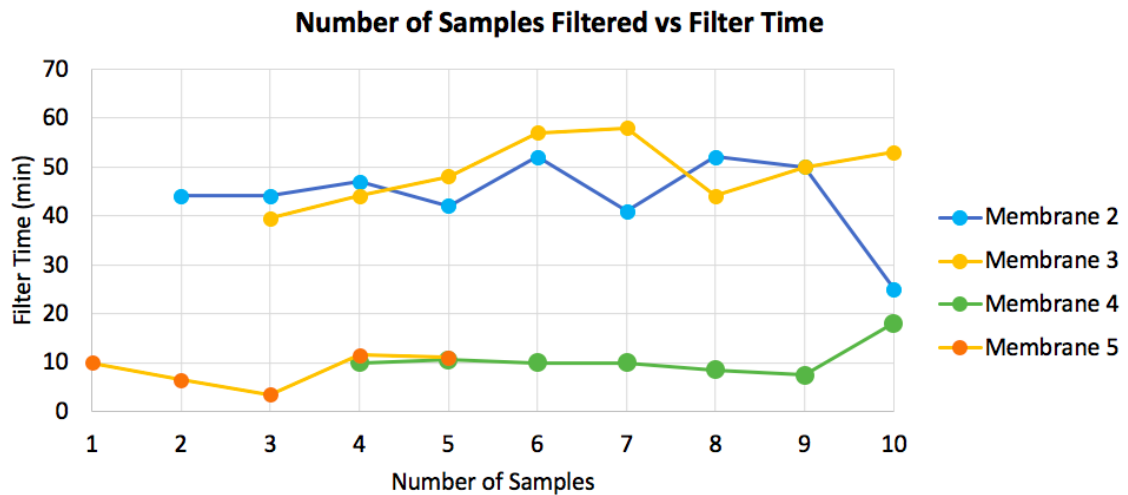


Figure 23: Number of samples filtered compared to filtration time.

4.2.1 Scanning Electron Microscopy

SEM was used to compare the surface of membranes at different stages in testing. SEM images illustrate changes on the surface of the membranes through different extents of lab testing. Three membranes were chosen to show surface affects at different stages in testing. Figure 23 shows the naked eye image of the three membranes imaged, with the

cut-out indicating the portion of the membrane removed for SEM analysis. Membrane 3B is functionalized and never used, membrane 5 is functionalized and used 5 times and membrane 2B is functionalized and used 12 times. Visually, there is very little difference between the three membranes, though 2B may show reduced density of CNTs across its surface compared to the others. Note that membranes 5 and 2B have scratches on their surface. These scratches were made after the last round of testing using either forceps or a glass pipet. They were chosen to be viewed using SEM because they were no longer suitable for testing due to these scratches.



Figure 24: Picture of membranes chosen for SEM imaging.

For SEM analysis, five images were taken for membranes 3B and 5, and two were taken for membrane 2B, at different spots on the membrane's surface to provide enough visual data to be representative of the membrane as a whole (12 pictures total). Note that the SEM used for testing was experiencing difficulties when taking images of membrane 2B,

so there are fewer images and they are of lower visual quality. Images from membrane 3B and 5 will primarily be used as a comparison due to their visual quality.

The MWCNTs embedded on membranes 3B, 2B and 5 are approximately 35nm in diameter and most are between 0.5 and 3 μm in length. The MWCNTs on membrane 3B range from straight to curly across the image. The MWCNTs on membrane 3B are opaque and densely packed together. (Figure 25 & 26)

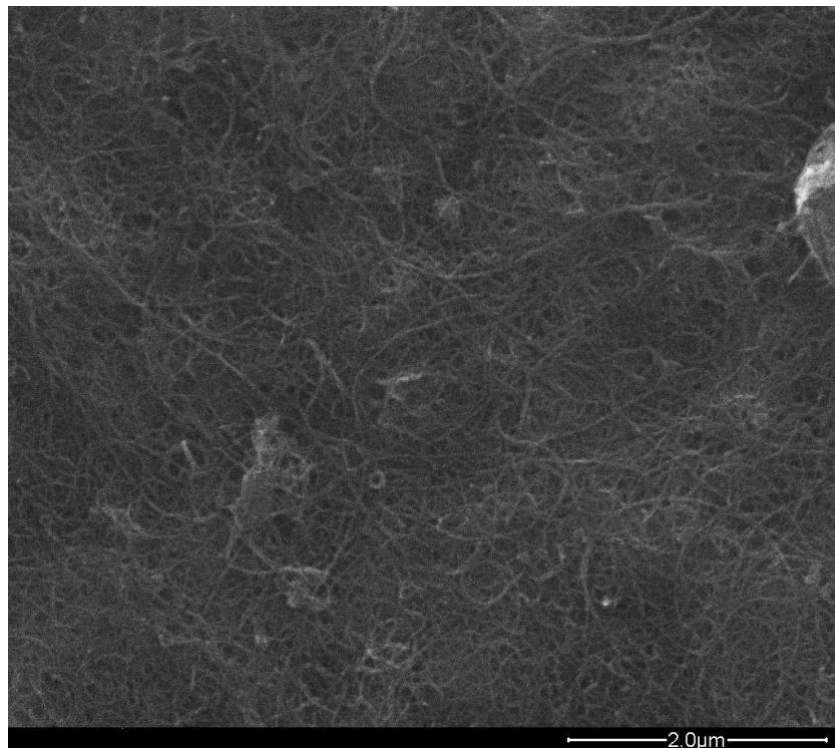


Figure 25: SEM image of membrane 3B, photo 2 of 5.

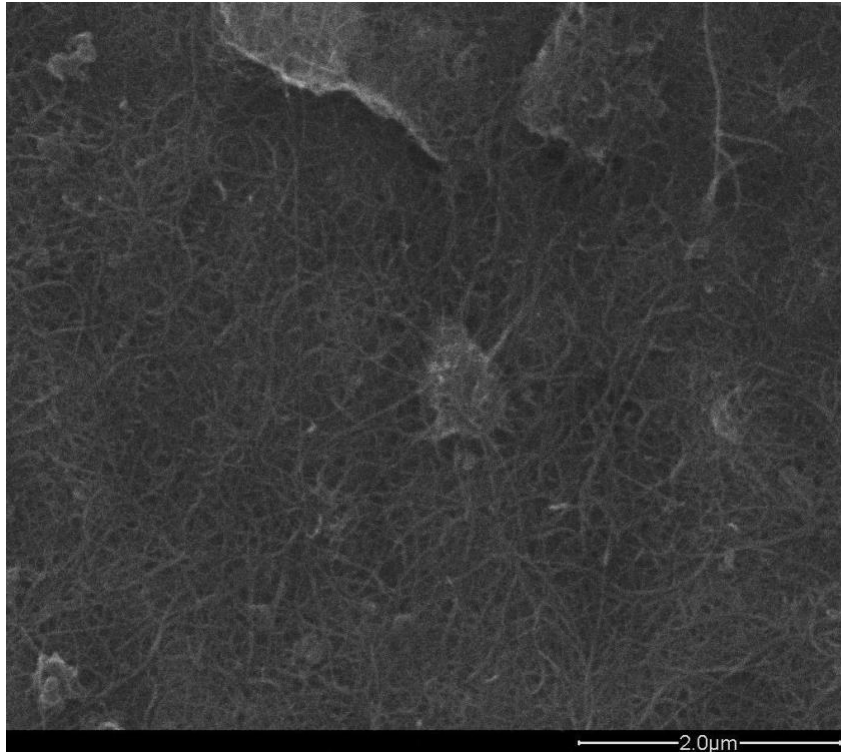


Figure 26: SEM image of membrane 3B, photo 1 of 5.

MWCNTs on membrane 5 and 2B range from straight to curly to jagged. There are various foreign objects on the right side of Figure 27. In addition, large spaces in-between the MWCNTs can be seen. The MWCNTs appear to be lighter, more translucent, which may indicate interior defects. With repeated use the surface of the membrane sees many changes, some of which improve treatment ability by creating more available active sites at surface defects. With extended filtration unidentifiable particulate matter appear on the surface and with extended use could potentially cause fouling. (Figure 27, 28 & 29) Further comparisons were not made between membrane 2B and 5 due to lack of representative images for membrane 2B.

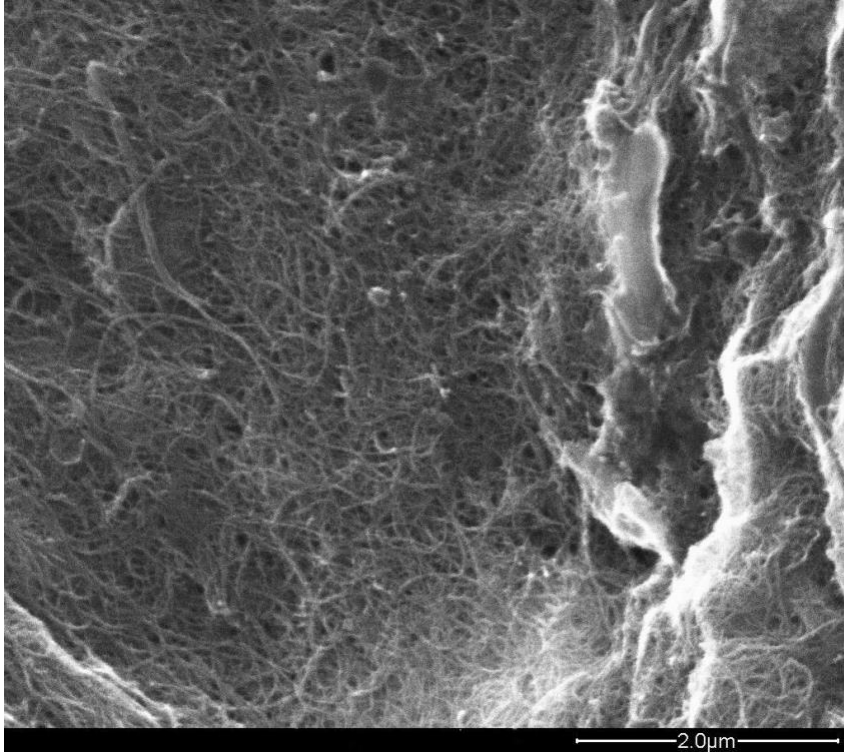


Figure 27: SEM image of membrane 5, photo 1 of 5.



Figure 28: SEM image of membrane 5, photo 2 of 5.

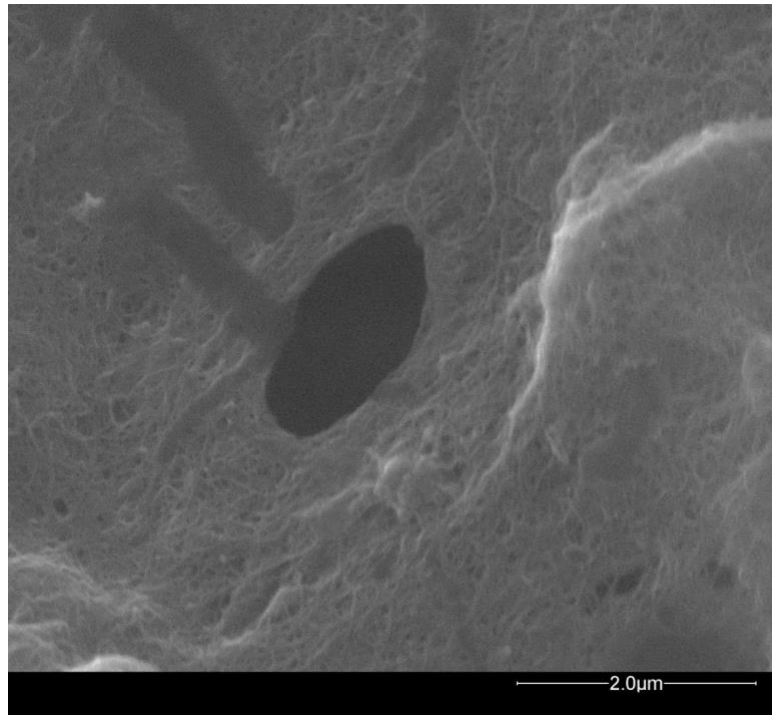


Figure 29: SEM image of membrane 2B.

SEM images can be used to see changes to the surface of the membrane and some changes to the MWCNTs themselves. TEM is an excellent tool to see internal changes to the MWCNTs. The surface of the MWCNTs on membrane 3B appear sleek and uniform, unlike 5 and 2B, “indicative of a uniform and largely defect-free sidewall structure” similar to the most far right image in Figure 30 [24]. All three membranes contain dense clusters of MWCNTs on-top and webbed into its surroundings, similar to those in the middle image of Figure 30. Densely packed structures will help decrease flow-through time and increase exposure time to both ozone and hydroxyl radicals. As discussed above, increased exposure time suggests higher percent removal. The surface of the MWCNTs on membrane 5 appear to be more uneven and irregular, similar to the middle image in

Figure 30. Defects on the surface of the MWCNTs are indicative of reductions in amorphous carbon as well as defects, “breaks,” on the outer surface of the MWCNTs [24].

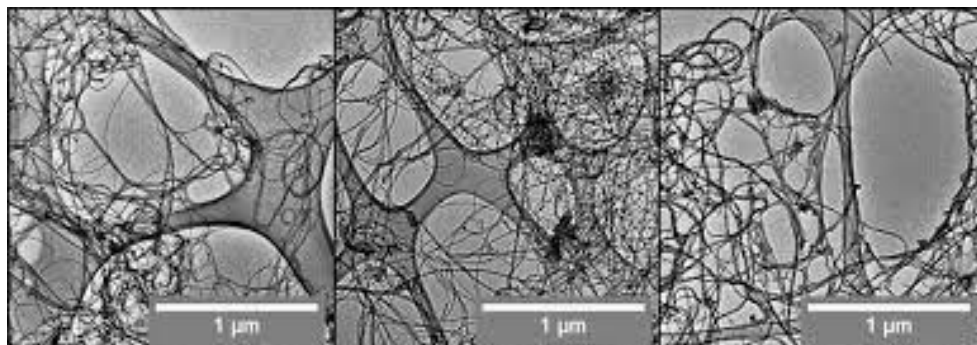


Figure 30: Low magnification TEM micrographs (left to right): pristine MWCNTs (0.9% O), O₃ treated MWCNTs (4.7% O), H₂SO₄/HNO₃ treated MWCNTs (10.2% O) [24].

It is difficult to see the surface irregularities with the limited magnification used for membranes 3B, 5 and 2B. Figure 31, copied from literature review, illustrates highly magnified MWCNTs after different levels of oxidation. The MWCNTs present on membrane 5 and 2B would most likely compare to the images on the right in Figure 31. Membrane 3 likely has fewer sidewall defects. Membranes 5 and 2B have received extended ozone exposure and will likely have developed extensive sidewall defects.

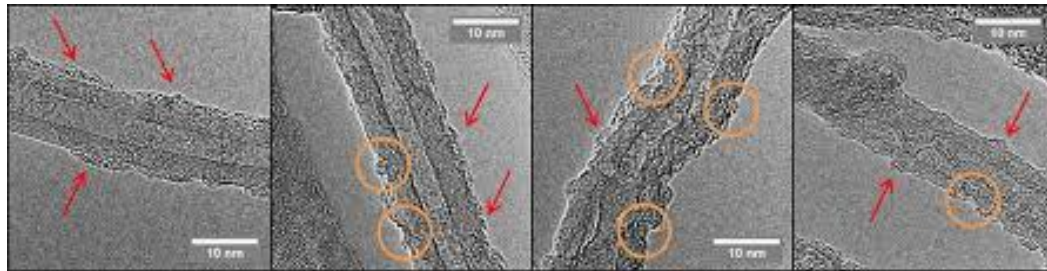


Figure 31: Representative TEM Micrographs (left to right): pristine MWCNTs (0.9% O), H₂O₂ treated MWCNTs (4.5% O), H₂SO₄/HNO₃ treated MWCNTs (5.1% O), KMnO treated MWCNTs (5.3% O). Amorphous carbon is indicated with arrows, sidewall defects highlighted by circles [24].

4.2.2 Filtration Time

Results from lab testing found a correlation between filtration time and percent removal. Two theories as to why filtration time may vary between membranes are differences in percent CNT loading on the membrane surface and or development of preferential pathways on the membrane surface.

Originally, running experiments using UV-Vis was motivated by the desire to analyze peak location as compared to those seen in the study conducted by Sahebian. The peaks were similar to those achieved by Sahebian but not definitive. More interestingly, UV-Vis results suggest a potential discrepancy in CNT loading across different membranes, which may explain the variation in filtration time. Figure 32 shows four tests, each performed using the same sonication and pipetting procedure described in the “Bucky Membrane” fabrication section above. There are two distinct clusters of data, both with similar trends across the wavelength spectrum measured, but with different levels of absorbance. These two clusters suggest that the samples had different CNT percent loading in solution; the

sample with higher absorbance likely had a higher percent loading. These results suggest that CNT loading is highly variable when pipetted following the fabrication procedure used in this study.

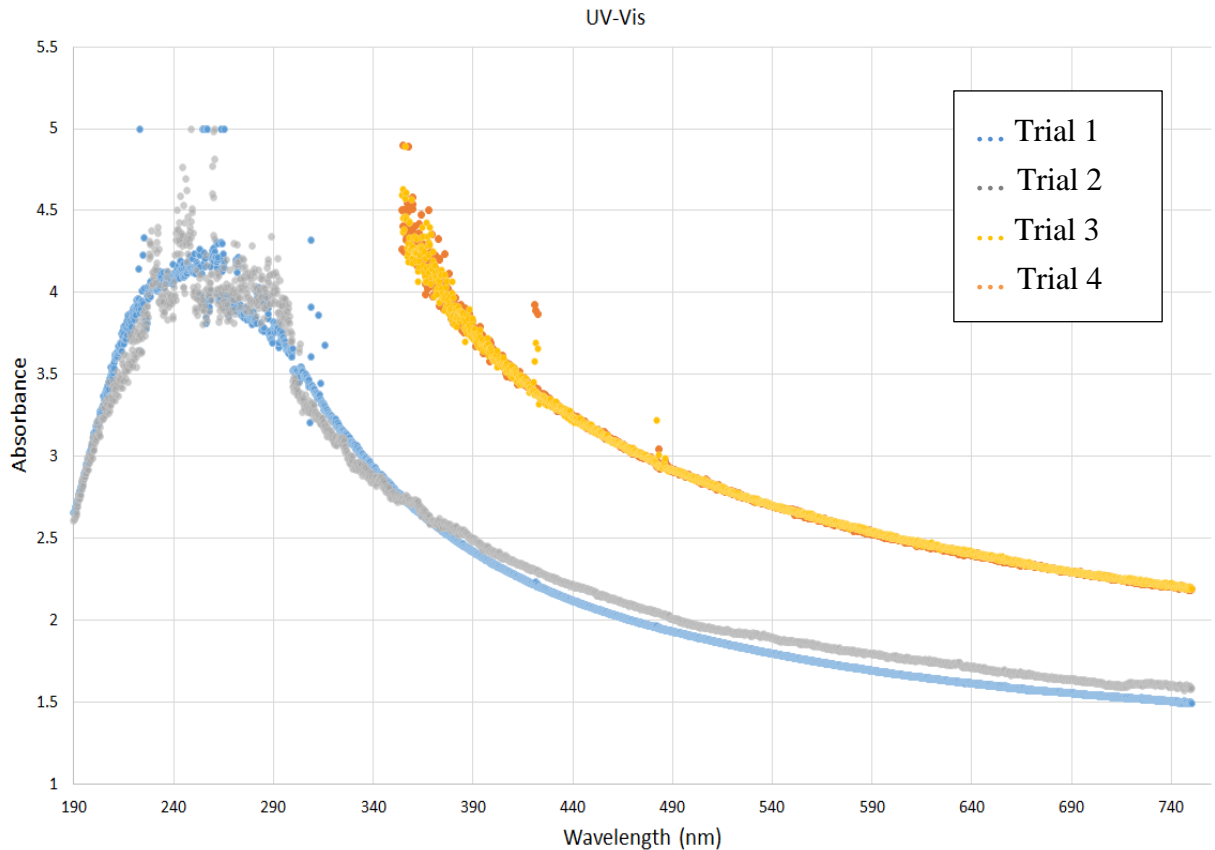


Figure 32: UV-Vis spectra from functionalized MWCNTs in solution.

Images from SEM illustrate possible preferential pathways on the surface of the membranes. Membrane 5 was used for five filtration tests (Figure 35 & 36) and membrane 2B was used for 12 filtration tests (Figure 33 & 34). Possible holes and cracks in the CNT layer on both surfaces have been circled. These CNT gaps might provide preferential pathways for water flow, allowing some of the water to pass through the filter with minimal CNT exposure. As preferential pathways form with repeated use of

the same filter, it would be expected that percent removal would decrease because of reduced oxidation time because water can pass more quickly through the membrane via the preferential pathways. Results from testing showed no strong correlation between the preferential pathways. Results from testing showed no strong correlation between number of tests performed and percent removal or flow through time. It is likely that the preferential pathways present on the membrane were made during membrane fabrication. Alternatively, the preferential pathways may have formed during treatment, however they comprised a small enough percentage of total surface area that they did not have a noticeable effect.

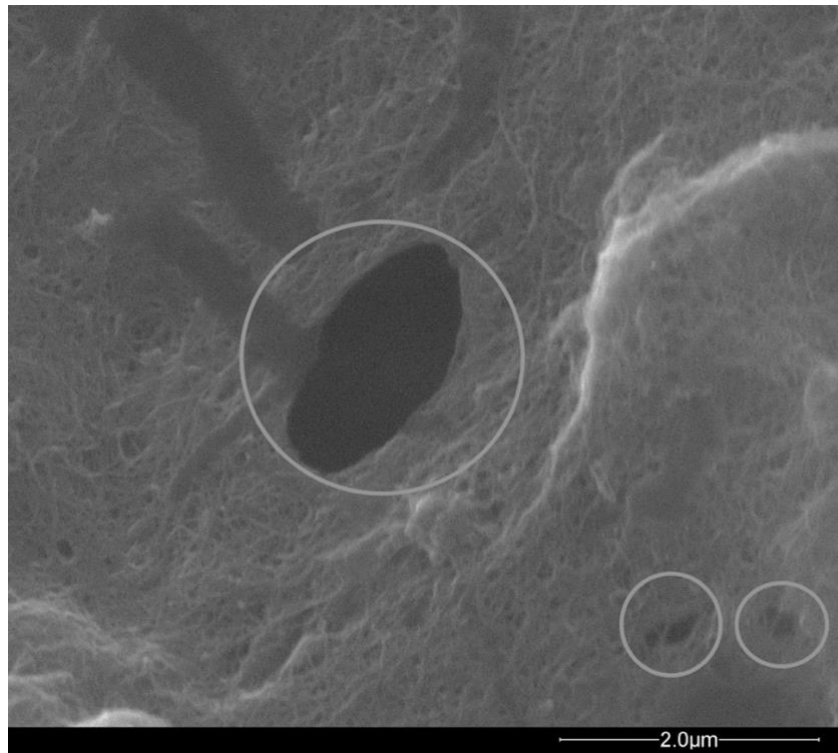


Figure 33: SEM image of membrane 2B, photo 1 of 2.



Figure 34: SEM image of membrane 2B, photo 2 of 2.

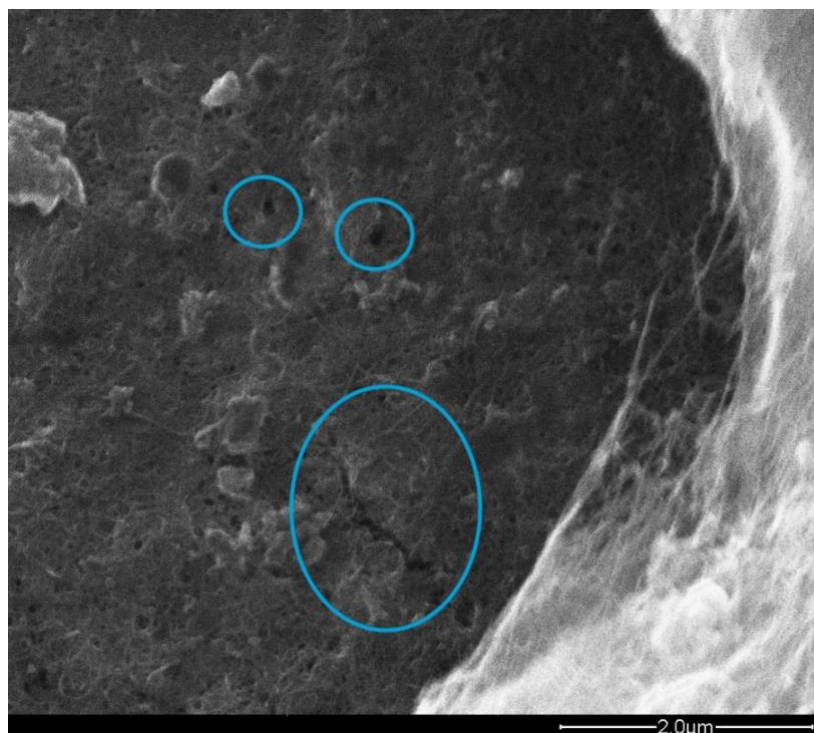


Figure 35: SEM image of membrane 5, photo 3 of 5.



Figure 36: SEM image of membrane 5, photo 2 of 5.

4.2.3 Total Ozone Exposure

Results from filtration lab testing indicate an increase in removal efficiency with extended ozone exposure. Extended ozone exposure is calculated using ozone absorbance and filtration time. The total ozone exposure is equal to the sum of absorbance with respect to time during each test. Figure 37 compares filtration time with ozone exposure; there is a general trend that as filtration time increases so does total ozone exposure. This makes sense since filtration time is a factor in ozone exposure and steady state ozone concentration was held within a specific range (list range) for all experiments.

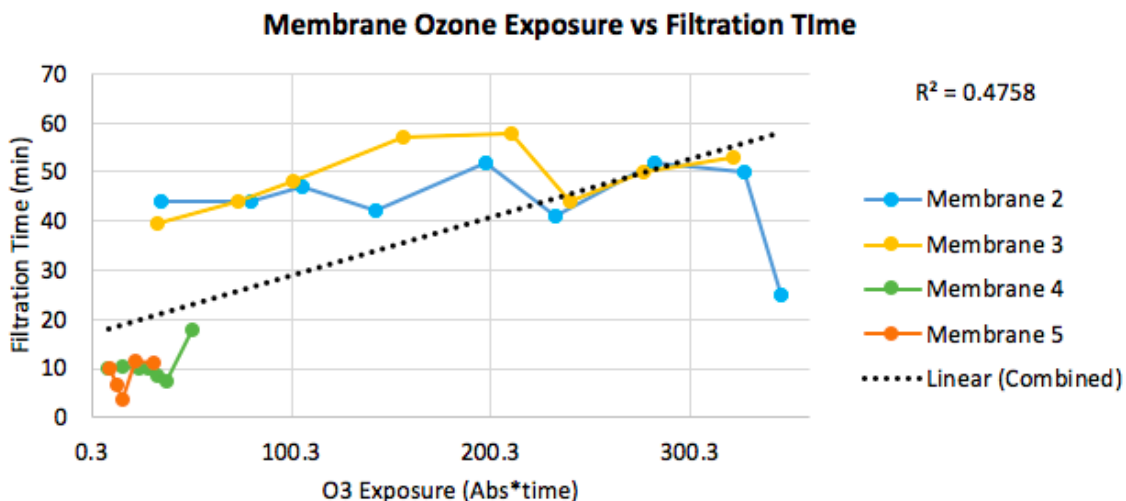


Figure 37: Membrane ozone exposure compared to filtration time.

Extended ozone exposure increases • OH production as well as the production of other functional groups including C=O by the CNTs and thus achieves greater contaminant removal [15]. SEM Images do show changes to the CNTs with extended exposure to ozone; however, they do not prove the presence of hydroxyl and carboxyl groups. Validating the presence of these functional groups on the CNTs was attempted using FTIR. FTIR was used to produce spectra for all membranes including: blank, functionalized, non-functionalized, 5, 10 and 12 run membranes. The blank membrane is illustrated in Figure 38, it was used as a means of calibration and comparison for the other membranes.

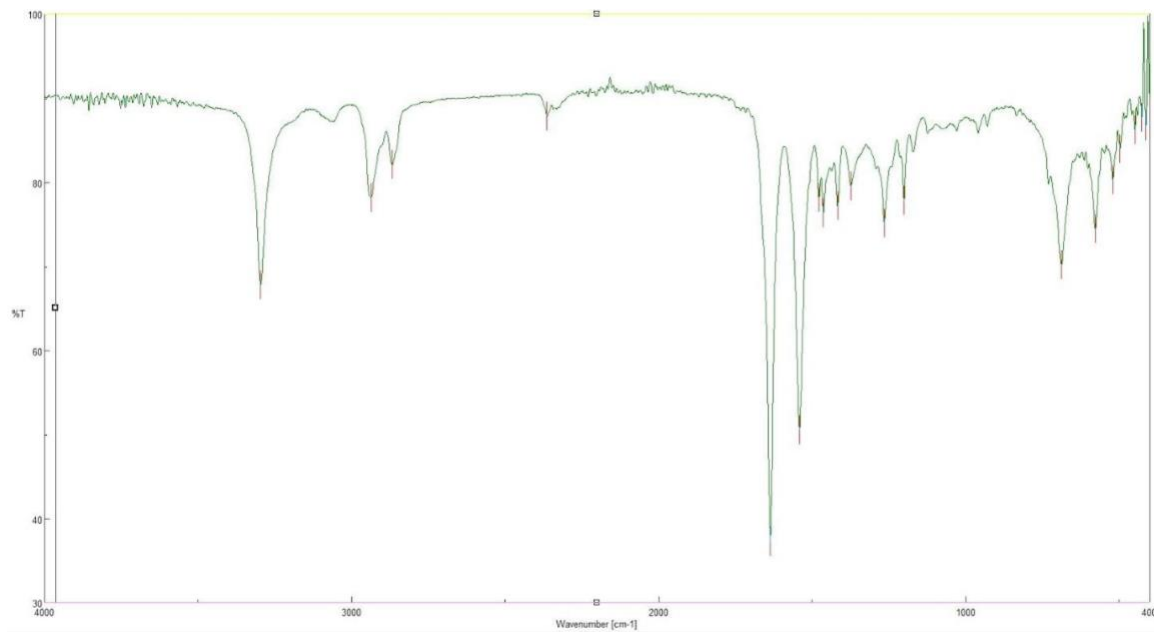


Figure 38: FTIR spectra of nylon membrane blank.

FTIR spectra between functionalized and non-functionalized membranes as well as those used for extended testing did not produce spectra with unique characteristics. Figure 39a was developed using membrane 4, fabricated with functionalized MWCNTs then used for ten filtration tests, and Figure 39b was of a non-functionalized membrane, however the peaks match. Peaks present on all other spectra seem to match despite their physical differences. Results suggest a similar outcome as was found in the Wespasnic study [24]. CNT loading was likely too high on the membranes to be measured using FTIR. Other forms of spectroscopy are recommended in the future to produce useable spectra.

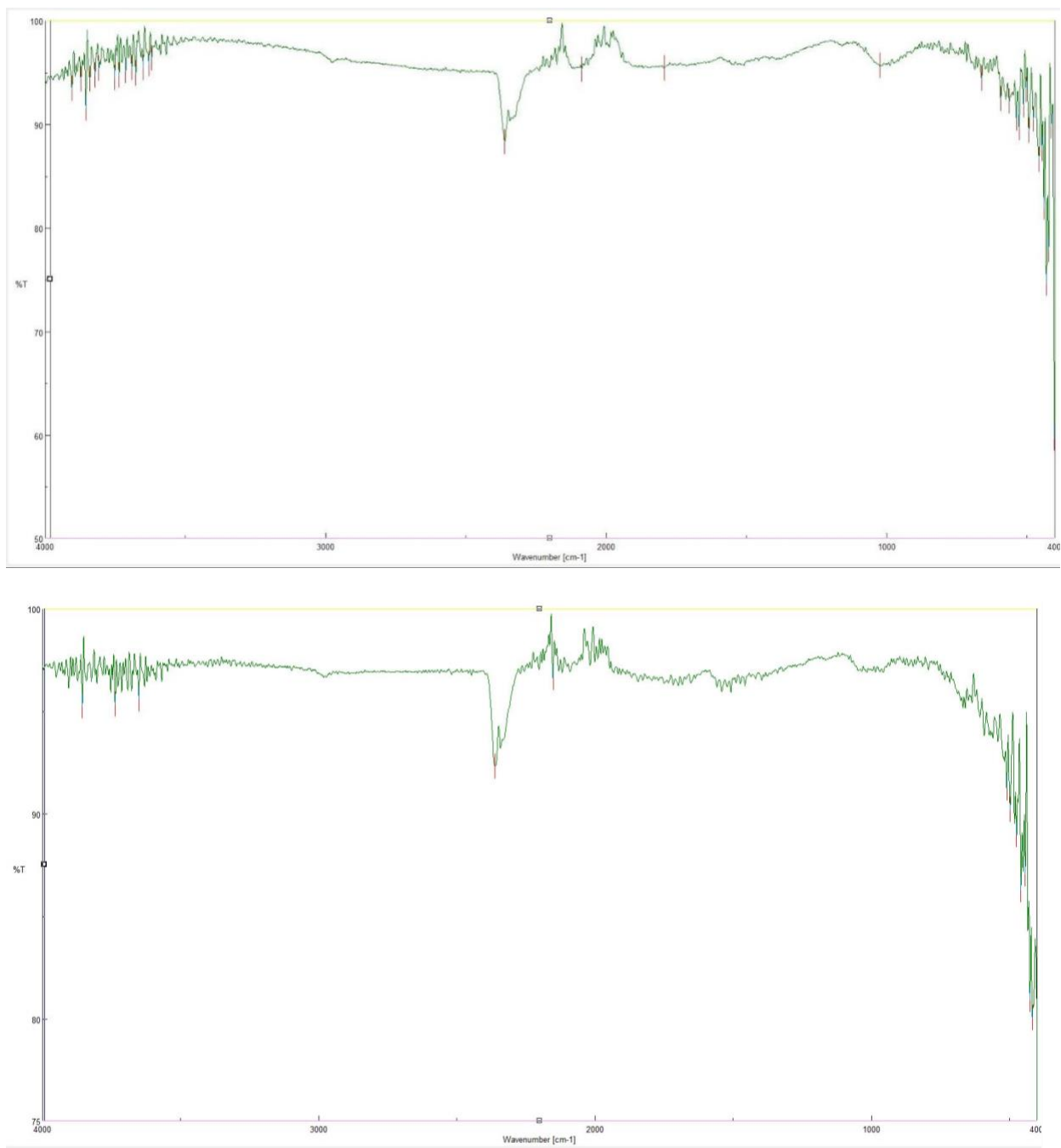


Figure 39: a) FTIR spectra of functionalized membrane 4 (top). b) FTIR spectra of non-functionalized membrane (bottom).

5. CONCLUSIONS AND FUTURE WORK

This thesis aimed to answer three questions regarding efficacy of ozonated CNT-enabled membranes for emerging contaminant removal.

The three questions motivating this study were:

- What experimental and operational variables affect percent contaminant removal during a single pass through a CNT-enabled membrane during ozonating conditions?
- How do the CNT-enabled membranes change with repeated uses and extended exposure to ozone, specifically regarding surface functionalization of the CNTs and integrity of the membrane itself?
- Can these results explain the variability of results between different membranes prepared under identical conditions?

These questions were explored using HPLC analysis of Atrazine degradation after passing through a CNT-enabled membrane during ozonating conditions. Membranes were used for multiple passes to explore effective longevity. HPLC analysis was supplemented with scanning electron imagery (SEM), Fourier Transform Infrared Spectroscopy (FTIR), Ultraviolet Spectrometer (UV-Vis) and comparison to published literature to provide additional insight into the experimental findings.

5.1 Percent Removal

Filtration tests were performed to determine the removal efficiency of MWCNT-embedded nylon membranes fabricated using the “Bucky Method”. Variables including

ambient temperature, ambient relative humidity, ozone absorbance in solution, filtration time, and number of samples filtered were measured to identify each membrane's performance, variability between membranes, and membrane longevity. Five membranes were used for testing; three performed ten rounds of tests, one performed 12 rounds of tests and one performed five rounds of tests. Ambient temperature and relative humidity did not seem to have any effect on ozone absorbance or percent removal. Tests were performed in an ice bath under a fume hood; in a full scale system operated outside of a lab, ambient temperature and relative humidity may have some effect on dissolved ozone concentration and consequently on percent contaminant removal. Results from testing suggest a relationship between ozone exposure and filtration time with percent removal. Ozone exposure was calculated for each solution filtered as well as total ozone exposure for each membrane. Percent removal was found to increase with extended exposure to ozone. Filtration times varied from 5 minutes to just under an hour. Results showed increased percent removal with increased filtration times. These results illustrate that as filtration time increases Atrazine has increased exposure to • OH, extended exposure will achieve greater removal.

5.2 Membrane Longevity

Results are somewhat inconclusive regarding the reactive longevity of MWCNT enabled membranes used as a catalysis for oxidation. Results indicate percent removal generally increases as total membrane ozone exposure increases. They showed that effective membranes remain effective for at least 10 passes, 26 mL treated per pass. Only one

membrane was used for more than 10 passes and showed a decline at the 12th pass. However, since only one membrane experienced that many repetitions the decline in productivity for the twelfth use does not constitute a conclusive finding.

SEM imaging was used to visually compare membranes after zero, five and twelve rounds of filtration. Results conducted using SEM identified holes in the surface of some membranes but not others. Preferential pathways created by the holes on the surface of the membrane would promote faster filtration times and reduced percent removal. However, findings did not indicate that these preferential pathways, if they did indeed exist, were causing significant changes in filtration time over repeated uses of the same filter. Filtration times showed no downward trends through each round of testing despite the presence of holes found on the filtered membranes. The holes found on the surface of the membranes may have been created during fabrication or over time during testing; either way, the holes showed no effect on membrane performance. In addition, SEM imaging illustrated changes in the shape and density of CNTs on the surface of the membrane, but these changes did not seem to affect membrane efficacy. Results show no sign of reduced performance with extended use. In the future, more tests, both experimental runs and spectroscopic analysis as described below, should be performed on the membranes to determine what the expected lifetime is of the membrane.

FTIR was used to compare the presence of functional groups on the surface of the membranes. Since ozone is an oxidant, it was expected the extended ozone exposure would increase surface functionality of the MWCNTs [15]. Results developed using FTIR spectra were inconclusive. Peaks present on spectra for non-functionalized and

functionalized membranes matched despite their different surface chemistries. Similar results were produced in a study performed by Wepsanik [24]. CNT loading was likely too high to use FTIR, future tests are recommended using a lower CNT surface loading.

5.3 Membrane Variability

Further testing was performed to try to determine why there was such a large variance between filters prepared using the same procedure. Unexpected findings while performing UV-Vis tests suggested a flaw in the procedure for preparing the membranes. Despite the use of sonication to evenly disperse the CNTs in solution, percent loading of CNTs in the pipette and onto the surface of the membranes is likely inconsistent. Percent loading is an important variable because it controls filtration time, ozone exposure and thus • OH production for each membrane.

5.4 Future Work

The successful design of a CNT-enabled membrane advanced oxidation process would open the door for new methods of CEC treatment. Further development and testing of the proposed design must occur before it can feasibly be implemented full scale.

5.4.1 Improved Membrane Fabrication Procedure

As discussed above, UV-Vis analysis highlighted a potential flaw in the procedure used to create membranes following the “Bucky Method.” Sonication was used as a means to break up aggregate clusters and evenly distribute the MWCNTs in solution prior to pipetting. However, CNT loading appears to have been inconsistent across the different

membranes, despite a consistency in fabrication procedure. To solve this problem, new methods of fabrication should be tested. A high sensitivity scale can be used before and after embedding the membranes with CNT to determine percent loading by weight for each membrane and ensure consistent CNT application on each membrane.

5.4.2 Further Membrane Longevity Testing

Once a more consistent method of fabrication is developed, all of the above experimental procedures should be repeated. Theoretically, filtration times and percent removal should be more consistent from one membrane to another once fabrication is improved. To learn more about membrane longevity, tests should be performed until percent removal shows consistent decline. The point of decline will be indicative of the effective life of the membrane. Once a point of decline has been reached, SEM and TEM imaging should be used to identify changes to the surface of the membrane. SEM is well suited to indicate issues with membrane integrity, and TEM can be used to look at the surface of individual CNTs to determine effects of extended ozone exposure.

As discussed above, results from FTIR were inconclusive, possibly because of high CNT loading on the surface of the membranes. In a study that experienced similar problems with FTIR, X-ray photoelectron spectroscopy (XPS) was recommended as another spectroscopy method [24]. Spectra taken using XPS should identify peaks indicative of oxygen groups expected to be present on the functionalized membranes.

5.4.3 Safety Concerns

One of the main safety concerns present when using MWCNTs is their potential threat to human and ecological health. MWCNTs are a known carcinogen shown to have

detrimental effects when inhaled [15]. Using a membrane fabrication process that embeds the CNTs into the membrane is meant to prevent MWCNTs from escaping as well as improve feasibility of implementation in a flow through system. While handling the membranes, MWCNTs have been removed via abrasives or contact with sharp objects. Once scraped off, MWCNTs become an additional contaminant. In addition, it is unknown CNTs are lost when water passes through the membrane, or if there are byproducts of the MWCNTs in the effluent solution. Research should be performed to determine if membrane degradation may be occurring or if the membrane-ozonation process may pose any substantial health risk to the environment.

5.4.4 The Future of Advanced Water Treatment

The goal of this study was to contribute to our understanding of MWCNT enabled AOPs. The use of MWCNTs as a catalysis for advanced oxidation has already been tested and proven as a viable treatment method. In order for this method to be suitable for full scale treatment, implementation in a flow-through system such as one with MWCNT-enabled membranes, must be tested and proven viable. As knowledge in the field of AOPs grows so does the ability to perform advanced water treatment and increase reuse of limited water resources.

REFERENCES

- [1] Rosenfeld, P. E., & Feng, L. G. H. (2011). Emerging Contaminants. In *Risks of Hazardous Wastes* (pp. 215–222). <https://doi.org/10.1016/b978-1-4377-7842-7.00016-7>
- [2] Stefanakis, A. I., & Becker, J. A. (2015). A review of emerging contaminants in water: Classification, sources, and potential risks. In *Impact of Water Pollution on Human Health and Environmental Sustainability* (pp. 55–80). <https://doi.org/10.4018/978-1-4666-9559-7.ch003>
- [3] Bai, X., Lutz, A., Carroll, R., Keteles, K., Dahlin, K., Murphy, M., & Nguyen, D. (2018). *Occurrence, distribution, and seasonality of emerging contaminants in urban watersheds*. <https://doi.org/10.1016/j.chemosphere.2018.02.106>
- [4] Contaminants of Emerging Concern including Pharmaceuticals and Personal Care Products | Water Quality Criteria | US EPA. (n.d.). Retrieved March 27, 2020, from <https://www.epa.gov/wqc/contaminants-emerging-concern-including-pharmaceuticals-and-personal-care-products>
- [5] Hill, R., & Scarisbrick, B. (1940). Production of oxygen by illuminated chloroplasts [3]. *Nature*, Vol. 146, pp. 61–62. <https://doi.org/10.1038/146061a0>
- [6] Regulations.gov - Supporting & Related Material Document. (n.d.). Retrieved March 27, 2020, from <https://www.regulations.gov/document?D=EPA-HQ-OPP-2003-0367-0318>
- [7] United States Environmental Protection Agency, “Results of the Lake Michigan Mass Balance Study: Atrazine Data Report,” Chicago, 2001.
- [8] *EPA Region 4 Human Health Risk Assessment Supplemental Guidance*. (2018). Retrieved from <https://www.epa.gov/risk/region-4-risk-assessment-contacts>
- [9] National Center for Biotechnology Information. PubChem Database. Atrazine, CID=2256, <https://pubchem.ncbi.nlm.nih.gov/compound/Atrazine> (accessed on Mar. 27, 2020)
- [10] Proposed pathway for degradation of atrazine by strain HB-6. (n.d.). Retrieved March 27, 2020, from

https://plos.figshare.com/articles/_Proposed_pathway_for_degradation_of_atrazine_by_strain_HB_6_/1175241

- [11] Metcalf, W., & Eddy, C. (2003). Metcalf and Eddy Wastewater Engineering: Treatment and Reuse. *Wastewater Engineering: Treatment and Reuse McGraw Hill. New York, NY.*
- [12] Buttiglieri G., Knepper T.P. (2008) Removal of Emerging Contaminants in Wastewater Treatment: Conventional Activated Sludge Treatment. In: Barceló D., Petrovic M. (eds) Emerging Contaminants from Industrial and Municipal Waste. The Handbook of Environmental Chemistry, vol 5 / 5S / 5S/2. Springer, Berlin, Heidelberg
- [13] Gómez-Espinosa, R. M., & Arizmendi-Cotero, D. (2019). Role of Membrane on Emerging Contaminant Removal. In *Handbook of Environmental Chemistry* (Vol. 66, pp. 157–174). https://doi.org/10.1007/698_2017_149
- [14] Coimbra, R., Escapa, C., & Otero, M. (2018). Adsorption Separation of Analgesic Pharmaceuticals from Ultrapure and Waste Water: Batch Studies Using a Polymeric Resin and an Activated Carbon. *Polymers*, 10(9), 958. <https://doi.org/10.3390/polym10090958>
- [15] R. L. Oulton, “Development of nanomaterial-enabled advanced oxidation techniques for treatment of organic micropollutants Recommended Citation,” University of Iowa, 2013.
- [16] Fukushima, S., Kasai, T., Umeda, Y., Ohnishi, M., Sasaki, T., & Matsumoto, M. (2018, January 25). Carcinogenicity of multi-walled carbon nanotubes: Challenging issue on hazard assessment. *Journal of Occupational Health*, Vol. 60, pp. 10–30. <https://doi.org/10.1539/joh.17-0102-RA>
- [17] Ihsanullah. (2019, January 31). Carbon nanotube membranes for water purification: Developments, challenges, and prospects for the future. *Separation and Purification Technology*, Vol. 209, pp. 307–337. <https://doi.org/10.1016/j.seppur.2018.07.043>
- [18] ir spectroscopy - Hayzel.molicommunications.com. (n.d.). Retrieved April 14, 2020, from <http://hayzel.molicommunications.com/ir-spectroscopy/>

- [19] *J. Chem. Educ.* 2008, 85, 2, 279, Publication Date: February 1, 2008, <https://doi.org/10.1021/ed085p279>
- [20] *FTIR Sample Techniques: Attenuated Total Reflection (ATR) - US.* (n.d.).
- [21] File:ATR-FTIR Spectroscopy.png - Wikimedia Commons. (n.d.). Retrieved March 27, 2020, from https://commons.wikimedia.org/wiki/File:ATR-FTIR_Spectroscopy.png
- [22] Infrared spectroscopy is a technique for identifying different possible functional groups of organic... | Functional group, Organic chemistry, Organic chemistry tutor. (n.d.). Retrieved March 27, 2020, from <https://www.pinterest.com/pin/624944885767761648/?lp=true>
- [23] Sahebian, S., Zebarjad, S.M., vahdati Khaki, J. et al. A study on the dependence of structure of multi-walled carbon nanotubes on acid treatment. *J Nanostruct Chem* 5, 287–293 (2015). <https://doi.org/10.1007/s40097-015-0160-3>
- [24] Wepasnick, K. A., Smith, B. A., Schrote, K. E., Wilson, H. K., Diegelmann, S. R., & Fairbrother, D. H. (2011). Surface and structural characterization of multi-walled carbon nanotubes following different oxidative treatments. *Carbon*, 49(1), 24–36. <https://doi.org/10.1016/j.carbon.2010.08.034>
- [25] Scanning Electron Microscopy - Nanoscience Instruments. (n.d.). Retrieved March 27, 2020, from <https://www.nanoscience.com/techniques/scanning-electron-microscopy/>
- [26] Tomova, A., Gentile, G., Grozdanov, A., Errico, M. E., Paunović, P., Avella, M., & Dimitrov, A. T. (2016). *Functionalization and Characterization of MWCNT Produced by Different Methods.* 129. <https://doi.org/10.12693/APhysPolA.129.405>
- [27] UV Vis Spectroscopy | UV Vis Spectroscopy Applications | Edinburgh Instruments. (n.d.). Retrieved April 30, 2020, from <https://www.edinst.com/techniques/uv-vis-spectroscopy/>
- [28] R. L. Oulton, "Pharmaceutical and personal care products in effluent matrices: A survey of transformation and removal during wastewater treatment implications

for wastewater management.” Journal of Environmental Monitoring. Received 18th March 2010.

[29] E. Miller, “DEGRADATION OF EMERGING CONTAMINANTS BY ADVANCED OXIDATION USING MULTI-WALLED CARBON NANOTUBES AND CONTINUOUS OZONE INJECTION.” California Polytechnic State University, San Luis Obispo, 2019.

[30] "Science for Environment Policy": European Commission DG Environment News Alert Service, edited by SCU, The University of the West of England, Bristol.

APPENDICES

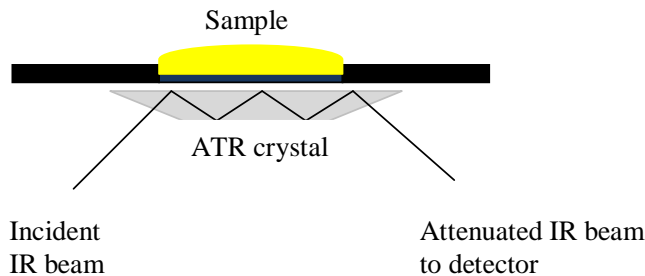
Appendix A: FTIR ATR Software Instructions

ATR protocol (JASCO FTIR-4100)

1. Introduction to ATR technique (Attenuated Total Reflectance)

While traditional IR spectrometers have been used to analyze solids, liquids and gases by means of transmitting the infrared beam directly through the sample, ATR uses the reflectance of the sample instead. An attenuated total reflection measures the change that occurs in a totally internally reflected infrared beam when the beam comes in contact with the sample. The infrared beam hits an optically dense crystal (*i.e.* diamond, zinc selenide or germanium) which then creates an evanescent wave that subsequently protrudes the sample (0.5-5 μm). The regions where sample absorbs energy, the evanescent wave will be altered, which will be detected.

It is important that the sample has good contact with the ATR crystal because the small extension of the evanescent wave beyond the crystal. This is accomplished by applying a moderate pressure to the sample during the measurement. Full and intimate contact of the sample onto the ATR crystal is essential to achieve high quality results. The refractive index of the crystal has to be significantly greater than the one of the sample.



While the analysis of samples by ATR is widely used, there are several factors that affect the quality of the final spectrum such as the refractive indices of the ATR crystal and the sample ($n_{\text{crystal}} > n_{\text{sample}}$), angle of incident IR beam, depth of penetration, wavelength of the IR beam, number of reflections, quality of the sample contact with ATR crystal, etc. The critical angle is given by

$$\theta_c = \sin^{-1} \left(\frac{n_{\text{sample}}}{n_{\text{crystal}}} \right)$$

For instance, a diamond/ZnSe system possesses a refractive index of $n_{\text{crystal}} = 2.4$ and a critical angle of $\theta_c = 38.7^\circ$. If the refractive index of the sample is higher than the refractive index of the crystal, derivative shaped absorbance bands are observed (see below) since the critical angle requirement was not met. The resulting spectrum is a mix of the ATR and external reflectance. The penetration depth is directly proportional to the wavelength of the incident beam, which means that photons with higher wavenumbers penetrate the sample less than photons with lower wavenumbers. Consequently, peaks on the left hand side often appear a little smaller than expected *i.e.* OH peaks, etc. It is important to correct this effect by applying the ATR correction to the raw spectrum.

General Pointers

- i. The FTIR instruments and the software located in YH1096, YH1111 and YH6076 are identical. The type and size of the crystals (first floor is ZnSe (~\$1200), sixth floor is a diamond crystal (~\$5000!!)) used in the ATR setup and the way the pressure is applied to the sample are a little different.
- ii. For 30BL, the first section of instruction period should consider any change to the micro-screw setting: 1.0 for powdery, 2.0 for smaller crystals and 3.0 for large crystals. Settings outside of this range will not improve the quality of the spectrum. Sample quantity (~10-20 mg) will be the most important and highly variable parameter.
- iii. For 30CL, no press screw adjustment is needed. The applied pressure has to be adjusted to the quantity and nature of the sample: the thicker the sample is the higher pressure should be in order to have better reflectance. Generally 20 mg of sample are sufficient. The high pressure clamp should be turned to its slip-clutch limit to achieve maximum pressure. In Chem 30CL, the pressure has to be released in order to be able to remove the clamp. If this is not done, the pin will hit the diamond crystal the next time it is placed on the sample and break it. You will receive a bill for the damaged crystal (\$5000+) due to the fact that you handled grossly negligent!
- iv. The setup should be cleaned using FisherBrand moist-wipe (lint-free wipes). The used wipes can be rinsed with acetone and save them in a box labeled "used wipes".
- v. The ATR has to be cleaned after each measurement. Keep in mind the film left over is often more reflective than the samples applied due to better contact, which can lead to false spectra. If unsure about the quality of the cleaning, a new background spectrum should be acquired prior to applying the sample to the crystal.

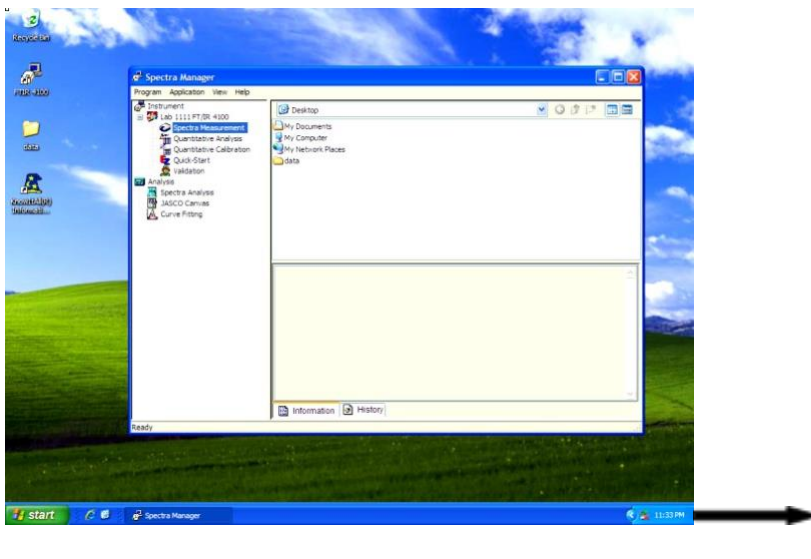
FTIR initialization (only necessary if you are the first one to measure the sample or the program has to be restarted)

- i. Turn on LCD monitor power (press any key on the keyboard usually). All programs/windows now open must be closed.
- ii. Turn on FTIR (switch on top). Double-click "FTIR 4100" icon.
- iii. Double-click "Spectra Measurement". This program manages several other programs, including for your purposes, "Spectra measurement" and "Spectra Analysis".

Cleaning the ATR module

- i. Scratching the crystal surface must be avoided at all cost!! It is expected some residual sample will be left. The TA will remove most of the remaining residual film before and after each meeting.
- ii. Much of the formed pellet can be dislodged with a wooden boiling stick. A metal spatula will be potentially too abrasive and damaging to the crystal. Students are not allowed to use them.

- iii. With the remaining solid at the edges, apply some acetone, dab the top with a FisherBrand wipe, and repeat this 4-5 times.
- iv. With acetone, moisten lint-free cloth provided by TA, and use this to scrub the general area in and around the crystal surface. It is not necessary to do this for more than a second or two. The solvent should not be applied in a way that the setup is soaked since it will leak into the optics as well.
- v. Remember to wipe the surface of the screw above.
- vi. The next background scan will subtract any remaining residue.



Acquiring the background spectrum

- i. Click “B” icon to acquire current background spectrum. The information window (see below) will pop-up. For the background spectrum, skip this by clicking “OK”. This will initiate the Spectra measurement program to acquire scans for background spectrum. This data will be sent automatically to the “Spectra Analysis” program.
- ii. The background spectrum should look like the ones below which only contains the CO₂ and the water peaks for the FTIR setup in the 1st floor (left side below). The right hand side shows the background spectrum for a diamond ATR setup, which shows additional peaks mainly in 1800-2300 cm⁻¹ range and at 1140 cm⁻¹ which are due to the diamond crystal.

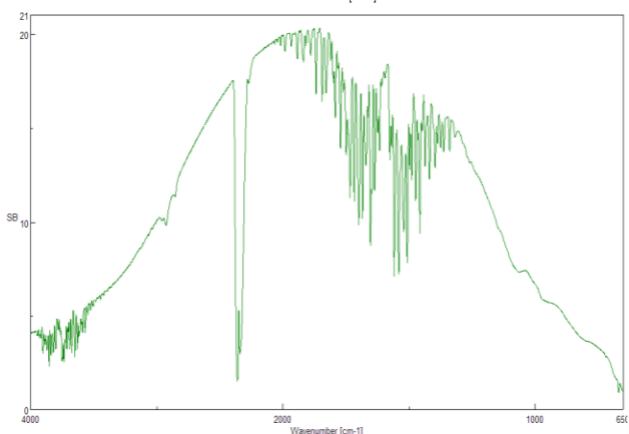
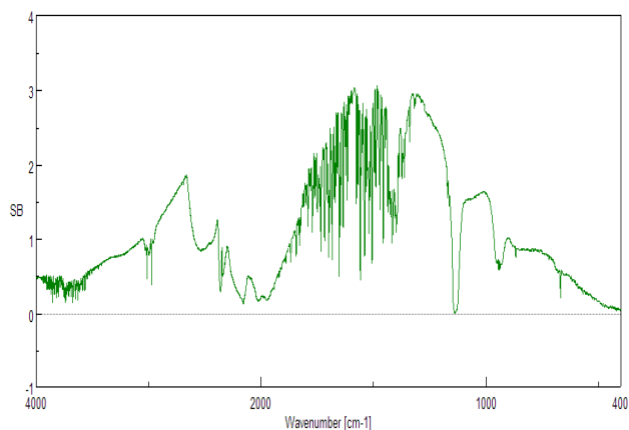
H₂O

H₂O CO₂

Sample setup on the ATR module

- i. Apply one drop or a small micro-spatula portion (15-20 mg) to fill the dwell 60-80% full (in Chem 30BL). Make sure not to scratch the crystal with the spatula.
- ii. Apply the press to the sample. The screw setting should usually not be changed.

- iii. In the “Spectra measurement” program click “S”. Enter your name and the name of your sample in the “Information” popup window.



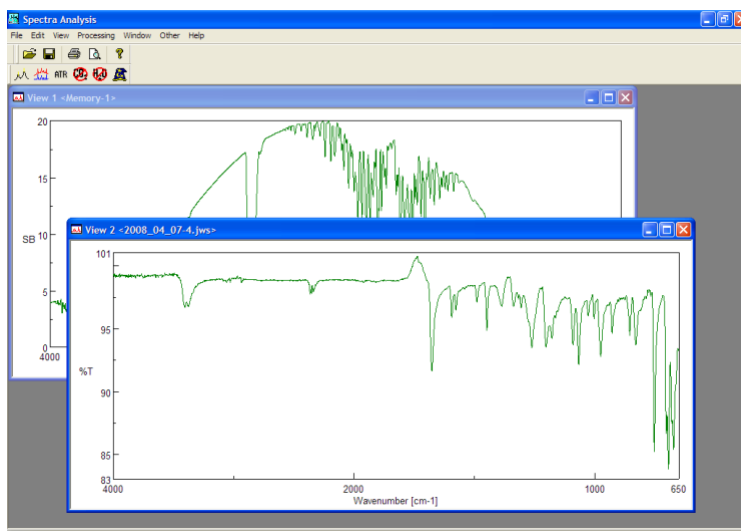
artifacts from diamond

The figure shows an "Information" popup window with a blue title bar and a close button (X). It contains four text input fields and two buttons at the bottom.

Sample :	benzoin
Operator :	Bacher
Division :	30BL
Comment :	April 7, 2008; 1 scoop

Buttons: OK, Cancel

- iv. Clicking OK will initiate data acquisition, Fourier transformation of the data, and transfer of the data to a new “View” window in the “Spectra Analysis” program.

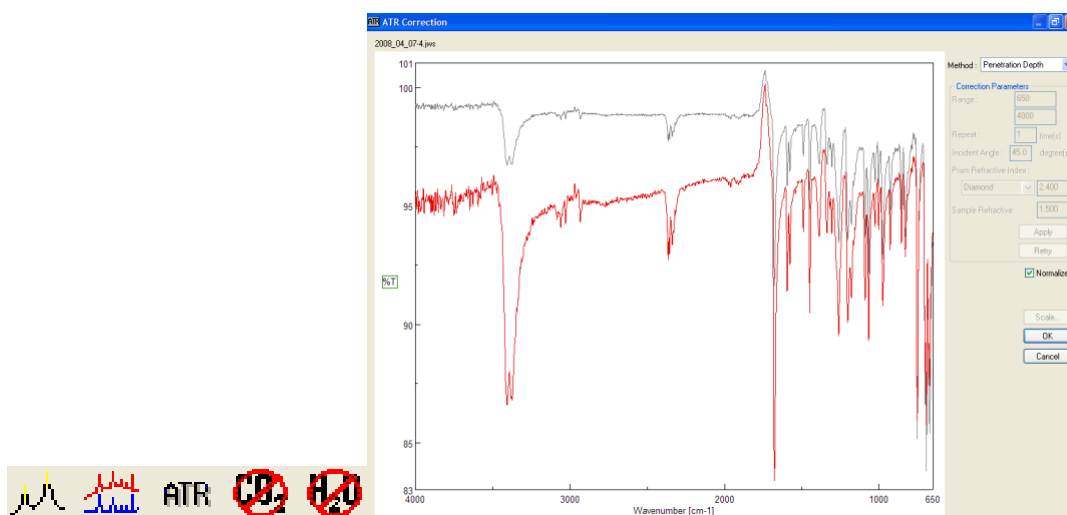


- v. If the signal is not appearing well enough above the noise, apply 5-10 mg more and try pressing the sample again.
- vi. A low amount of sample also gives rise to artifacts in the FTIR spectrum (~1100 (as strong peak) and 1740 cm^{-1} (often as inverted peak)).

Data Processing

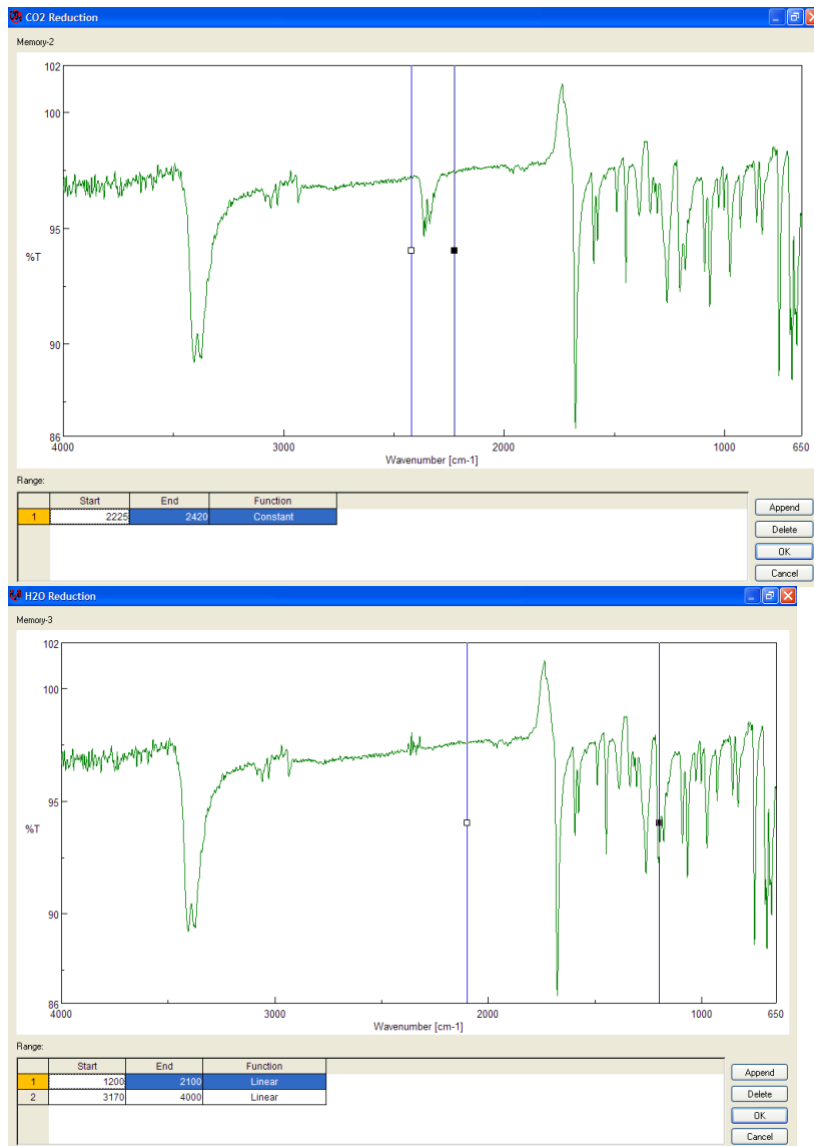
Here are the buttons that are going to be used for the data processing:



- i. In Spectra Analysis, click the “ATR” button (3rd button), click OK, and a 2nd “View” window pops up. Note that the peaks on the left side increased in size.

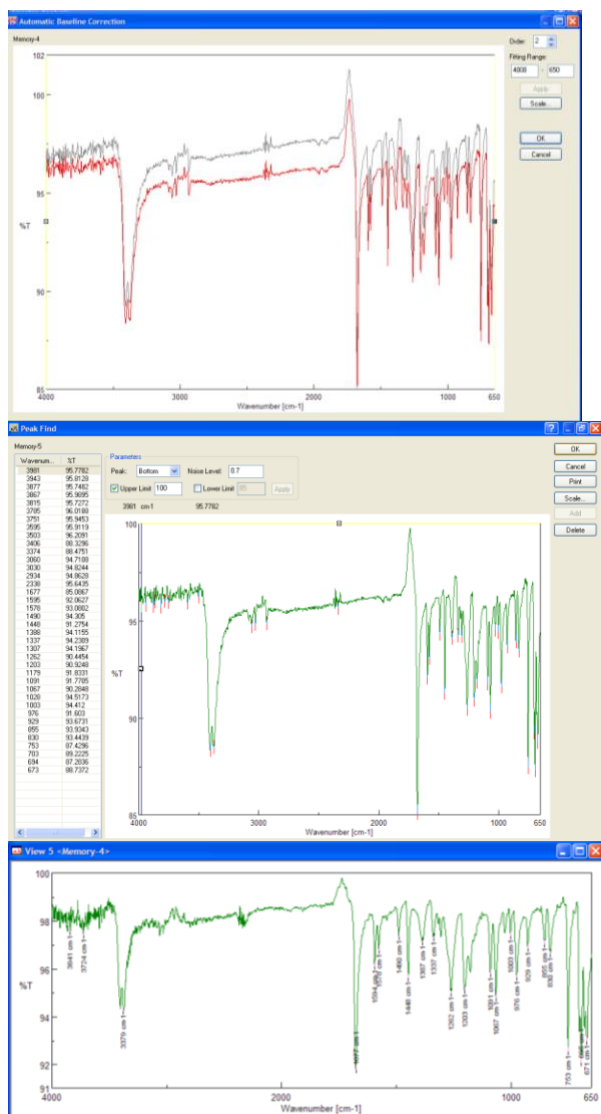


- ii. Click the “CO₂” button (4th button), click OK, and a 3rd “View” window pops up. Note that the peaks in the CO₂ window disappeared.
- iii. Click the “H₂O” button (5th button), click OK, and a 4th “View” window pops up.

Note: This step might have to be performed twice in order to remove the water peaks from both ranges.



- iv. Click “Automatic Baseline Correction” . Click OK, and a 5th “View” window pops up.
- v. Click the “Peak Find” icon . The noise level can be adjusted by either choosing the upper and lower limit numerically or by dragging the appropriate horizontal lines in place. Click “Apply.” Additional peaks can be added by dragging the vertical line to the peak and then clicking the “Add” button. Click OK, and a 6th “View” window pops up. (Do not print from this screen!)
- vi. Click the “print” icon. The attached printer will print the spectrum with the user name, entered sample information and the numbers right at the peaks.
- vii. Close all “View” windows, clicking “no” when prompted to save the data.



e. General remarks

Independent from the technique that is used, the IR spectra should be obtained in the range from 500-4000 cm^{-1} (for organic compounds). The background should be checked first before the spectrum of the compound is acquired. The new generation of FTIR spectrometer allows processing the data electronically, which usually leads to an improved quality of a spectrum using background correction techniques.

The laboratory course uses IR plates made from AgCl. Keep in mind that these plates are very expensive (~\$150). The compound should not react with them (strong oxidizing or reducing reagent?). If you check them out from the TA (in exchange for your ID card), it is your responsibility to return them in proper condition (clean and complete!). They are cleaned with dry acetone and Kim wipes, and not with water, alcohol and the brown or white paper towels! (Why?) AgCl plates have to be stored a closed box, protected from light, because they are light sensitive.

The IR samples should be prepared at the workbench, and not at or on top of the IR instrument. We encountered problems in past, because students spilled chemicals inside the instrument, which caused 'wrong' spectra and serious damage to the instrument, which cost \$\$\$\$.

Appendix B: Percent Removal Results Including all Membrane 6 Values

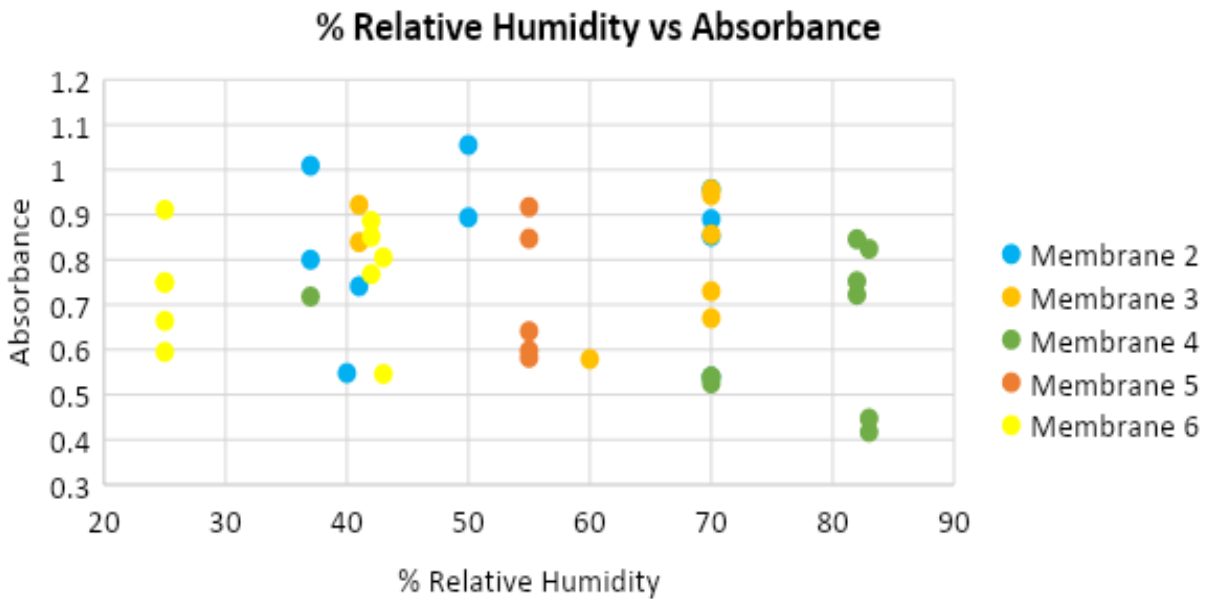


Figure B-1: Percent relative humidity compared to ozone absorbance.

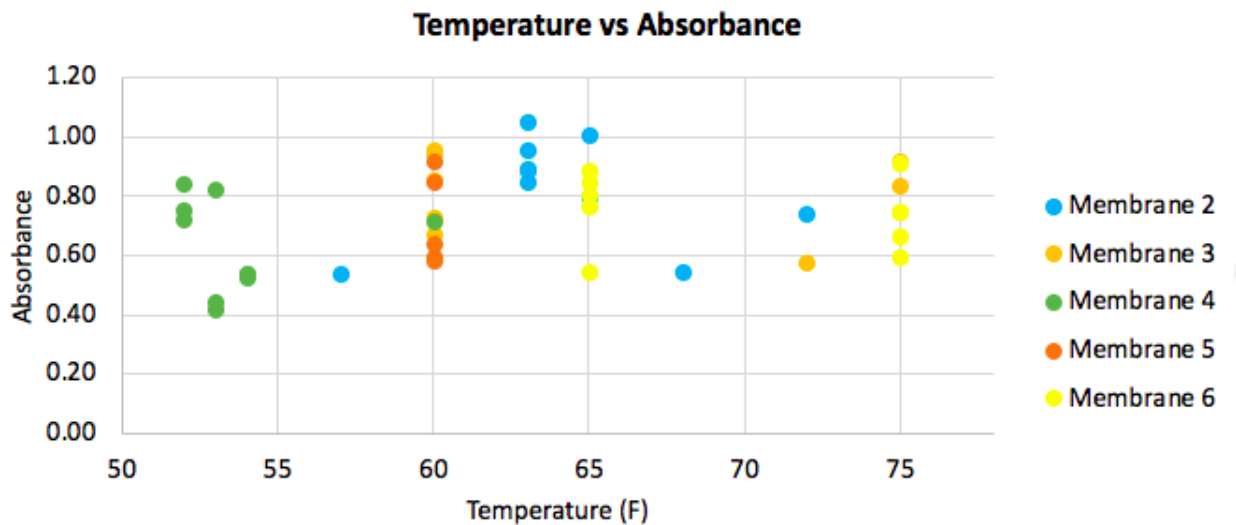


Figure B-2: Ambient temperature compared to ozone absorbance.

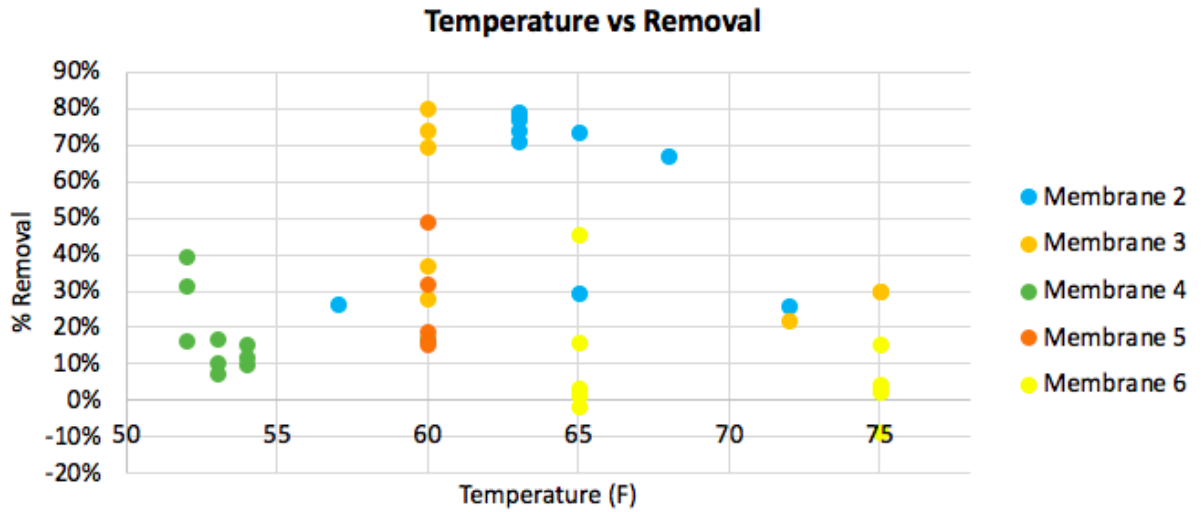


Figure B-3: Ambient temperature compared to percent contaminant removal.

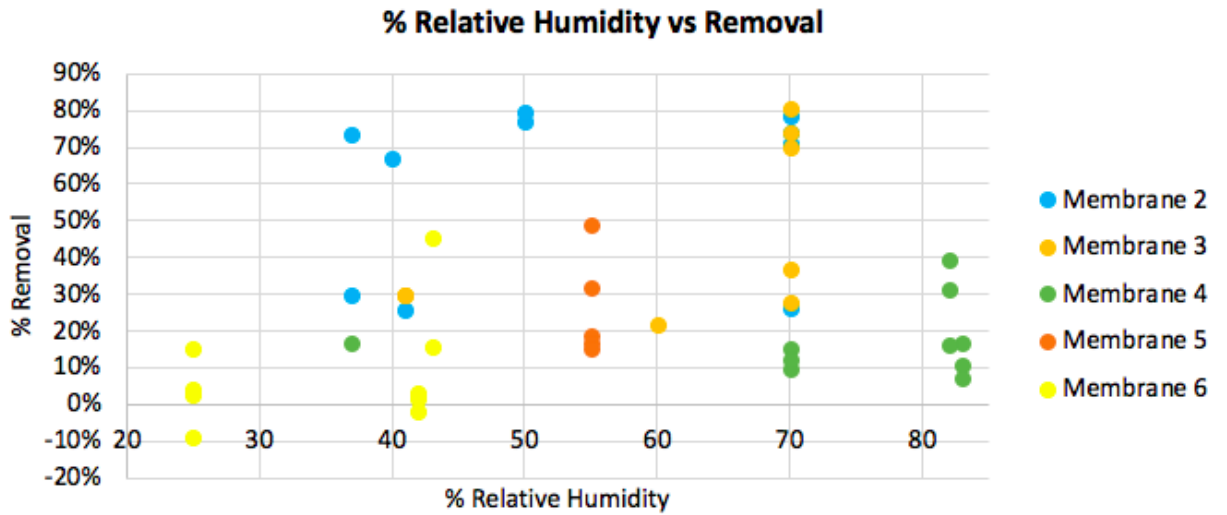


Figure B-4: Percent relative humidity compared to percent contaminant removal.

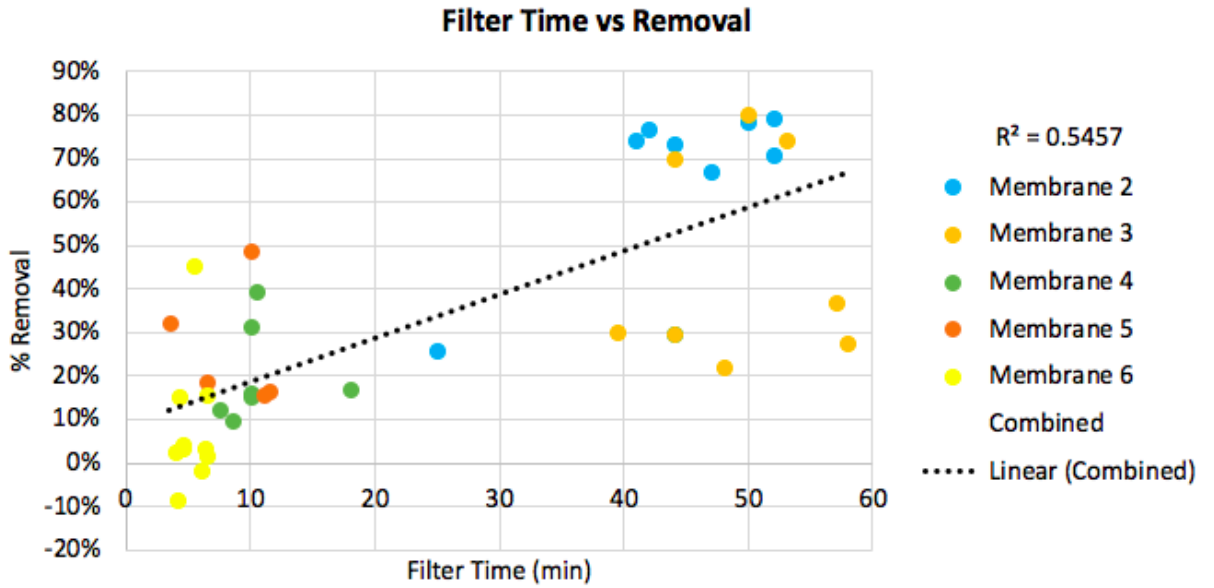


Figure B-5: Filtration time compared to percent contaminant removal.

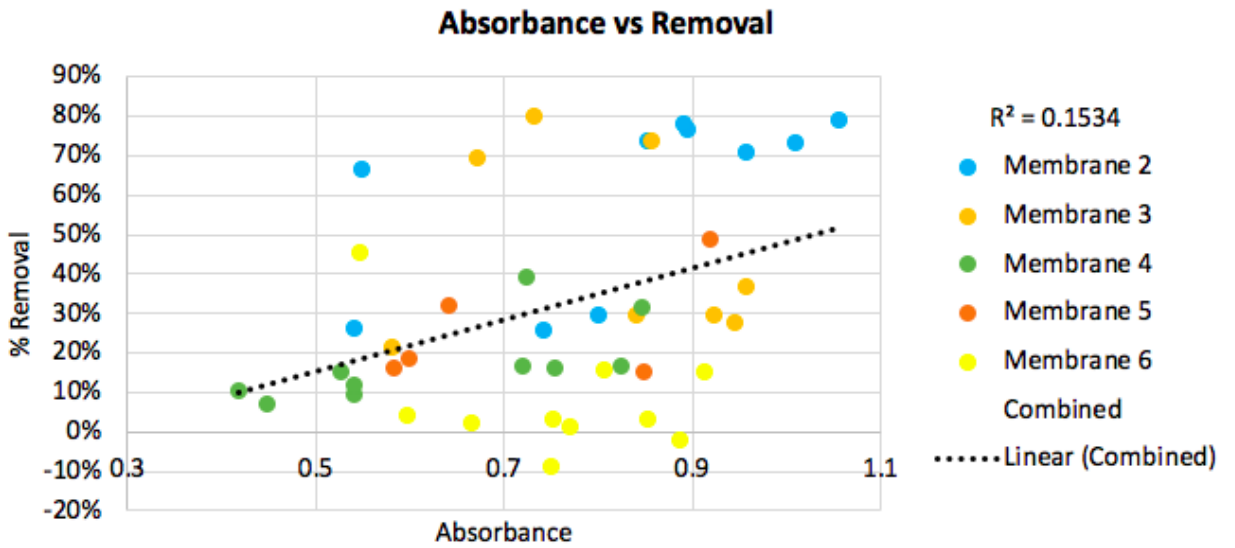


Figure B-6: Ozone absorbance in solution compared to percent contaminant removal.

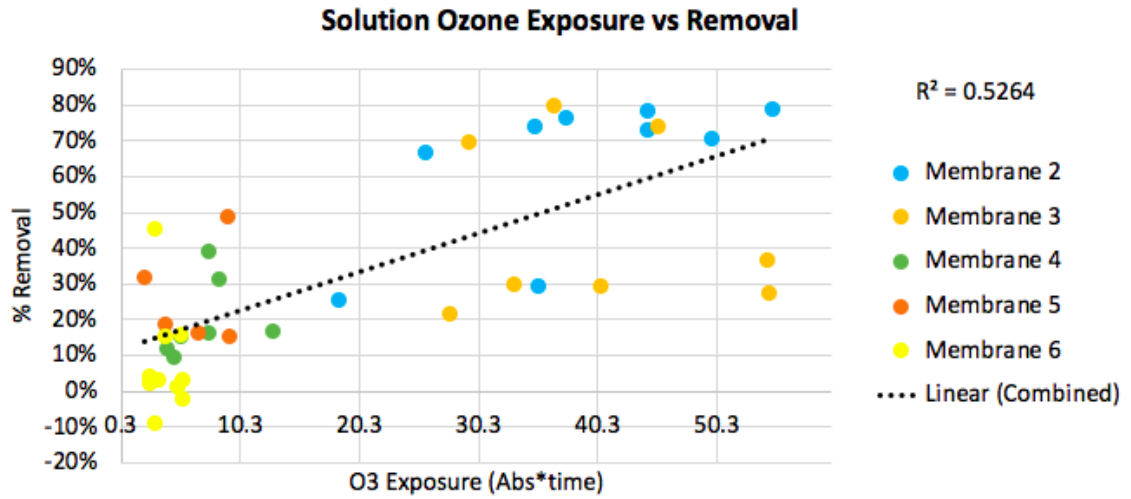


Figure B-7: Ozone exposure in solution compared to percent contaminant removal.

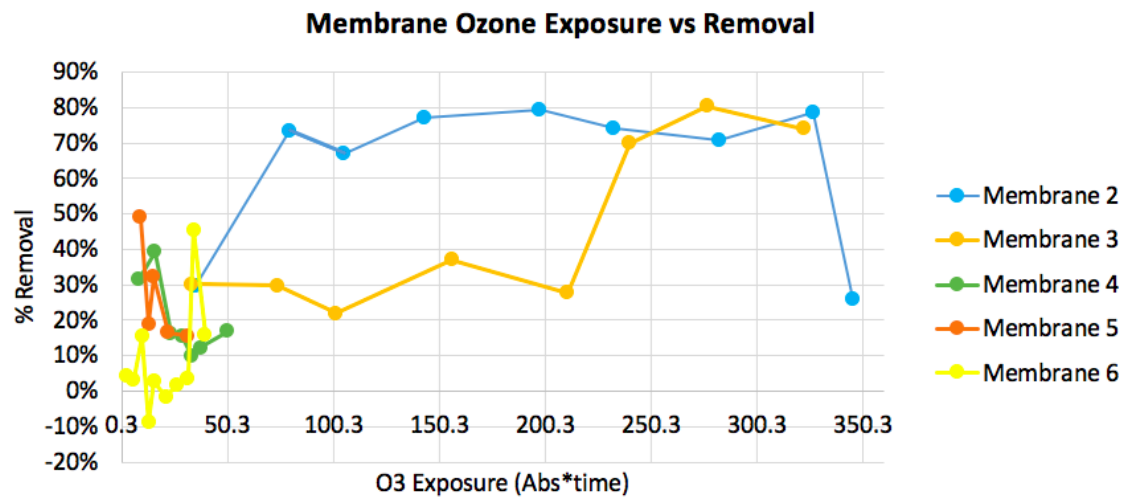


Figure B-8: Ozone exposure over the life of the membrane compared to percent contaminant removal.

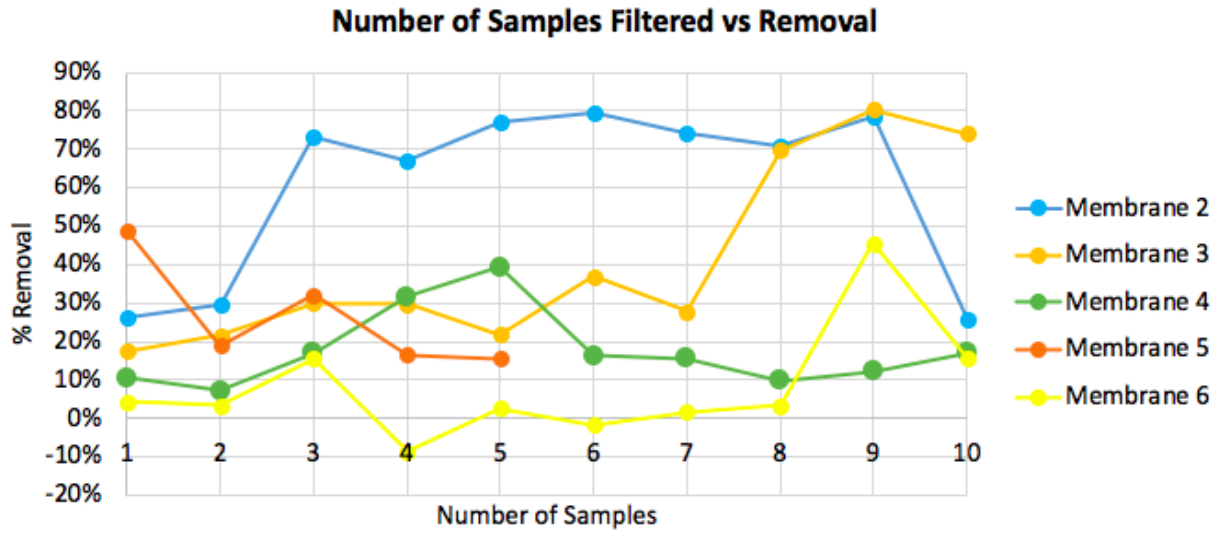


Figure B-10: Number of samples filtered compared to percent contaminant removal.

Appendix C: Additional SEM Images of Membrane 3B and 5.

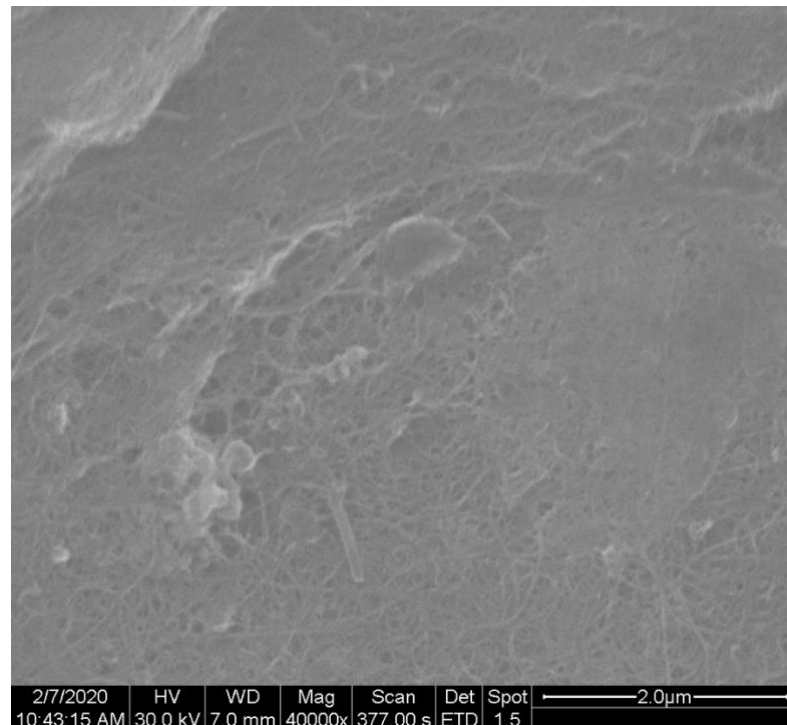


Figure C-1: SEM image of membrane 5, image 4 of 5.

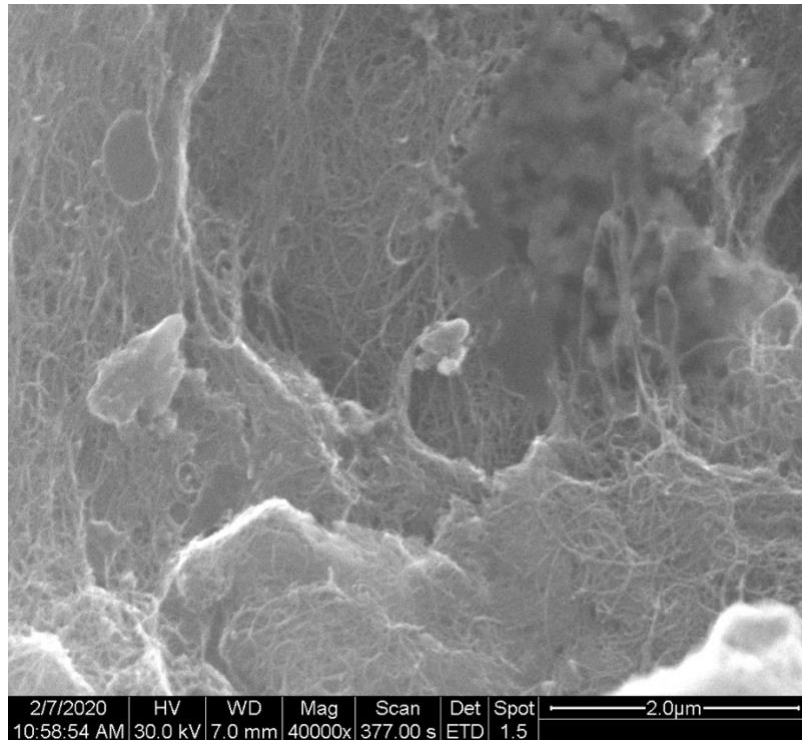


Figure C-2: SEM image of membrane 5, image 5 of 5.

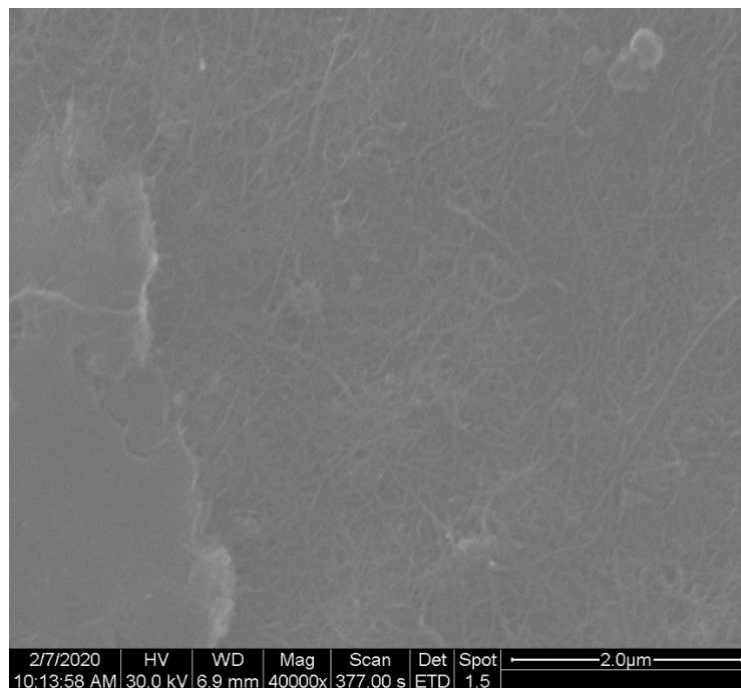


Figure C-3: SEM image of membrane 3B, image 3 of 5.

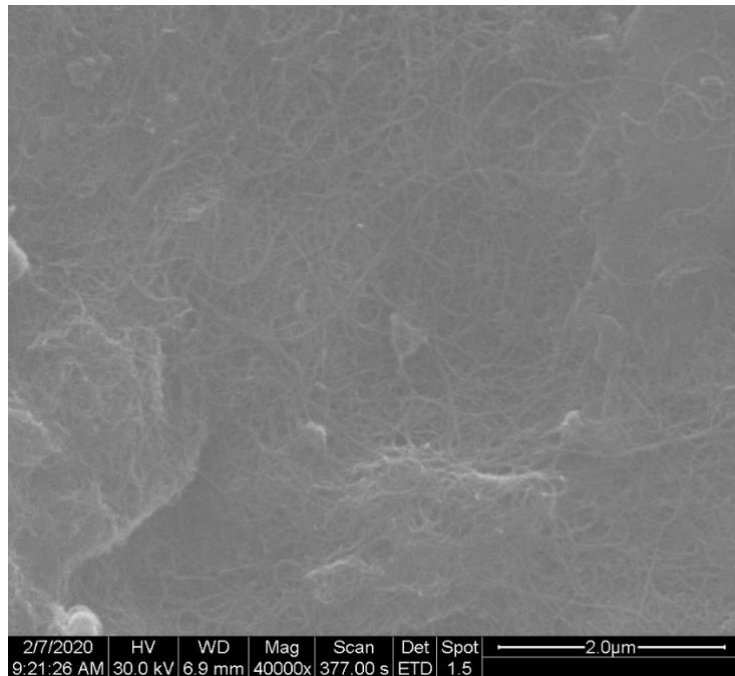


Figure C-4: SEM image of membrane 3B, image 4 of 5.

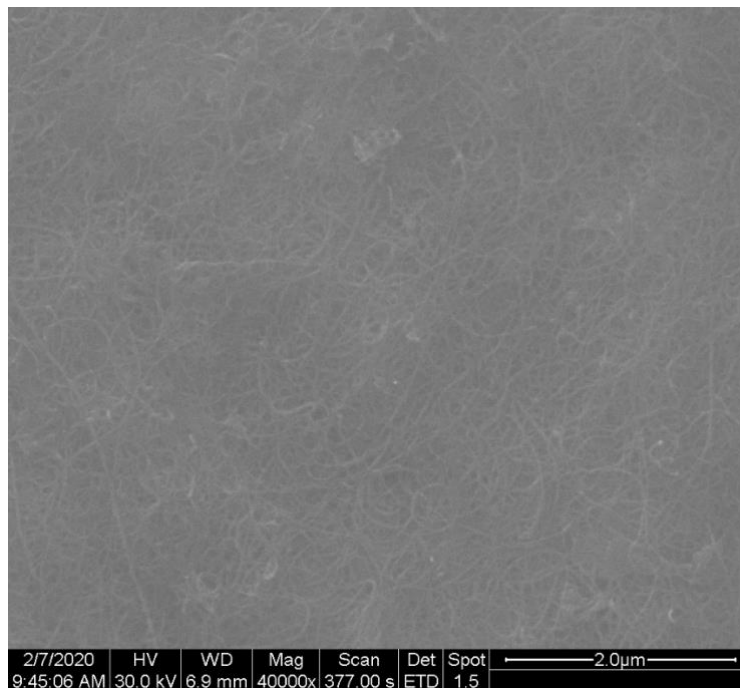


Figure C-5: SEM image of membrane 3B, image 5 of 5.